DOI: 10.1002/ejic.200600022

Synthesis, Structures and Catecholase Activity of a New Series of Dicopper(II) Complexes of Reduced Schiff Base Ligands

Bellam Sreenivasulu,[a] Fei Zhao,[b] Song Gao,[b] and Jagadese J. Vittal*[a]

Keywords: Biomimetic studies / Copper / Reduced Schiff-base complexes / Tridentate ligands / Catecholase activity / Magnetic properties

A series of dinuclear Cu^{II} complexes of reduced Schiff bases from substituted salicylaldehydes and amino acids have been synthesized and characterized. They are: $[Cu_2(RScp11)_2(H_2O)_2]$ {$H_2RScp11$ = 1-[(2-hydroxy-5-R-benzyl)amino]cyclopentane-1-carboxylic acid; R = H (**1**), Cl (**2**), CH_3 (**3**), OH (**4**)}, $[Cu_2(RSch11)_2(H_2O)_x]$ {$H_2RSch11$ = 1-[(2-hydroxy-5-R-benzyl)amino]cyclohexane-1-carboxylic acid; R = H and *x* = 1 (**5**), R = Cl and *x* = 2 (**6**), R = CH_3 and *x* = 2 (**7**)}, $[Cu_2(RSch12)_2(H_2O)_2]$ {$H_2RSch12$ = 2-[(2-hydroxy-5-R-benzyl)amino]cyclohexane-1-carboxylic acid; R = H (**8**), CH_3 (**10**) and $[Cu_2(ClSch12)_2]\cdot 2H_2O$ (**9**)}, $[Cu_2(Diala5)_2(H_2O)_2]\cdot H_2O$ [H_3Diala5 = *N*-(2,5-dihydroxybenzyl)-L-alanine] (**11**), $[Cu_2(Diala4)_2(H_2O)_2]\cdot H_2O$ [H_3Diala4 = *N*-(2,4-dihydroxybenzyl)-L-alanine] (**12**), and $[Cu_2(Diala3)_2(H_2O)_2]\cdot H_2O$ [H_3Diala3 = *N*-(2,3-dihydroxybenzyl)-L-alanine] (**13**). They were isolated and characterized by chemical and spectroscopic methods. Single crystal X-ray crystallographic studies have revealed that $[Cu_2(Scp11)_2(MeOH)_2]$ (**1a**), $[Cu_2(ClScp11)_2(DMF)(H_2O)]\cdot MeCN$ (**2a**), $[Cu_2(MeScp11)_2(MeOH)_2]\cdot 2MeOH$ (**3a**), $[Cu_2(ClSch11)_2(MeOH)_2]\cdot 2MeOH$ (**6a**), $[Cu_2(ClSch12)_2]\cdot 2MeOH$ (**9a**), and $[Cu_2(Diala4)_2(DMSO)_2]\cdot 2DMSO\cdot 2$acetone (**12a**) have 1D hydrogen-bonded polymeric structures while **4** has a 3D hydrogen-bonded network structure. Complex **8** displays a 2D coordination polymeric network structure. The complexes **1**–**13** have been investigated as functional models for the catechol oxidase by employing 3,5-di-*tert*-butylcatechol as a model substrate. Electron-withdrawing substituents reduced the activity while electron-donating substituents enhanced the activity. Variable-temperature magnetic studies conducted on compound **8** suggest the presence of strong inter-dimer antiferromagnetic coupling.

Introduction

Among the well-known representatives of Type III copper proteins, catechol oxidase with active dicopper(II) sites is a ubiquitous enzyme in living systems for catalyzing the oxidation of a wide range of *ortho*-diphenols to *ortho*-diquinones. The subsequent auto polymerization of the highly active quinones into polyphenolic catechol melanins is considered to be responsible for the defense mechanism observed in plants against pathogens or pests.[1] In fact, the two copper atoms of dicopper(II) bio-active centers present in different metalloenzymes are found to act cooperatively within the proximity of ca. 3.5 Å with each Cu^{II} center coordinated by three histidine donors.[2,3] As confirmed by the recent X-ray crystal structure analysis, catechol oxidase in the *met* oxidized form contains dicopper centers with a Cu···Cu distance of 2.9 Å.[3] Modeling the features of bio-relevant dinuclear active sites through synthetic analogues basically involves the judicious design of binucleating ligands to meet the conditions such as bridging mode controlling the metal–metal distance, steric-electronic properties, and geometry around the metal centers.[4] Consequently, dinuclear copper(II) complexes of the binucleating ligands have been extensively documented as bimetallic catalysts due to their potential ability to mimic the functions of the so-called catechol oxidase.[2,4–5]

Our research group has been interested in the coordination chemistry of reduced Schiff-base ligands, *N*-(2-hydroxybenzyl)-amino acids, which have the potential to form dinuclear complexes through a bridging phenolate group. In addition, these ligands can also afford the choice of coordination environments that determine the nature of metal ions that can be bound within the closest proximity. Apart from the studies illustrating interesting solid-state supramolecular transformation of Cu^{II} and Zn^{II} complexes,[6] and the novel helical stair-case structure in the Ni^{II} complex,[7] our research group has reported several dicopper(II) complexes derived from reduced Schiff bases as functional models for catechol oxidase.[8] Very recently, we have also demonstrated that the dicopper(II) complexes containing the weakly coordinating sulfonate donor group are more active

[a] Department of Chemistry, National University of Singapore, Science Drive 3, Singapore 117543
Fax: +65-6779-1691
E-mail: chmjjv@nus.edu.sg
[b] College of Chemistry and Molecular Engineering, Peking University,
Beijing 100871, P. R. China
Supporting information for this article is available on the WWW under http://www.eurjic.org or from the author.

catalysts towards the oxidation of 3,5-DTBC compared to their carboxylate analogues.[9]

In this paper, we report a new series of dicopper(II) complexes of reduced Schiff-base ligands formed between various substituted salicylaldehydes and aminocyclopentane/cyclohexanecarboxylic acids and L-alanine (Scheme 1). Our previous studies discussing the effect of chelating side arms[8] and the weakly coordinating sulfonate group[9] on the activity, prompted us to investigate and evaluate the activity of these closely related yet distinct series of dicopper(II) complexes with substituted phenyl rings under similar experimental conditions. Despite the plethora of reports on catecholase activity of various dicopper(II) complexes, studies modulating the activity in terms of electronic properties via substituted bridging phenolates have not been well documented.[10] Such an investigation of the structure-reactivity patterns is essential to enhance the mechanistic understanding of the parameters affecting the catecholase activity. In this paper, we present the salient structural features and the details of catecholase activity of the dicopper(II) complexes of various reduced Schiff-base ligands containing the substituted phenolate moiety. Further, variable temperature magnetic studies of a selected complex have also been discussed.

Results and Discussion

Copper complexes **1**–**13** have been synthesized in good yields by the complexation of Cu^{II} salts with the corresponding reduced Schiff-base ligands according to the procedures described in the experimental section. Owing to their poor solubility in common solvents except in DMF and DMSO, our attempts to obtain single crystals of the

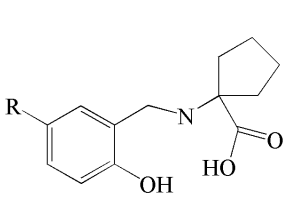

R = H, H_2Scp11
R = Cl, H_2ClScp11
R = Me, H_2MeScp11
R = OH, H_2(OH)Scp11

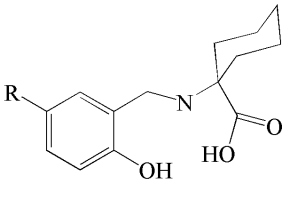

R = H, H_2Sch11
R = Cl, H_2ClSch11
R = Me, H_2MeSch11

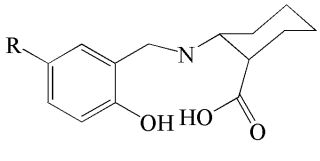

R = H, H_2Sch12
R = Cl, H_2ClSch12
R = Me, H_2MeSch12

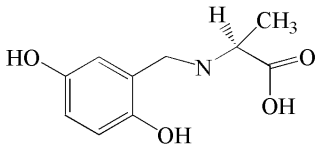

H_3Diala5

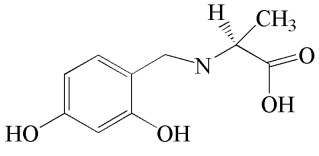

H_3Diala4

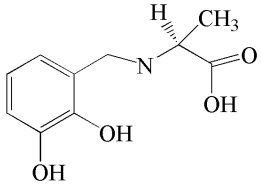

H_3Diala3

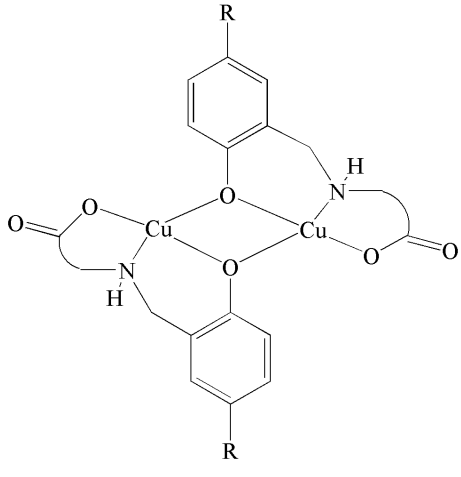

R = H, Cl, OH, CH_3

Scheme 1. Ligands and schematic diagram of dicopper(II) complex.

bulk as such were not successful. However, the single crystals obtained were different from the bulk due to lattice and coordinated solvents in the case of $[Cu_2(Scp11)_2(MeOH)_2]$ (**1a**), $[Cu_2(ClScp11)_2(DMF)(H_2O)]\cdot MeCN$ (**2a**), $[Cu_2(MeScp11)_2(MeOH)_2]\cdot 2\,MeOH$ (**3a**), $[Cu_2(ClSch11)_2(MeOH)_2]\cdot 2\,MeOH$ (**6a**), $[Cu_2(ClSch12)_2]\cdot 2\,MeOH$ (**9a**), and $[Cu_2(Diala4)_2(DMSO)_2]\cdot 2\,DMSO\cdot 2\,acetone$ (**12a**); however, complexes **4** and **8** afforded single crystals that were the same as the bulk during single crystal growth.

The IR absorption bands of the newly synthesized complexes **1**–**13** in the range of 3398–3458 cm^{-1} indicate the presence of coordinated or lattice water molecules in the compounds.[11a,11c] This can be further supported by the weight loss observed in thermo gravimetric (TG) analysis. The sharp bands observed in the range of 2927–2960 cm^{-1} are due to ν(N–H). The absorption bands observed in the region of 1597–1640 and 1360–1460 cm^{-1} are due to the asymmetric [$\nu_{as}COO^-$] and symmetric [ν_sCOO^-] stretching frequencies of the carboxylate group, respectively. The difference (Δν) between the asymmetric and symmetric stretching frequencies of carboxylate groups can be used to determine their binding mode in the metal complexes.[11a] In general, Δν for monodentate carboxylate is greater than 200 cm^{-1} and for a bridging carboxylate Δν is less than 200 cm^{-1}.[12] This observation has been confirmed for the 2D coordination polymeric structure in **8** showing the bridging ($\Delta\nu$ = 115) mode of carboxylate.

The initial weight loss in TG of **4** in the temperature range of 134–177 °C corresponds to the two water molecules coordinated to the Cu^{II} ions, which is corroborated by the crystal structure of **4**. The complex **8** showed weight loss for all six water molecules in the temperature range 80–119 °C and the crystal structure of **8** contains two aqua ligands and four lattice water molecules. The loss of metal bound water molecules along with lattice waters is similar to the observed behavior during the solid-state supramolecular transformations via thermal dehydration.[6a–b] The TG of the bulk **1**–**3**, **5**–**7**, and **9**–**10** showed weight loss in the temperature range of 60–168 °C due to the loss of two metal-bound aqua ligands. The observed dehydration temperature below 120 °C for **11** and **12**, and 130 °C for **13** also suggests similar behavior of metal bound aqua ligands as in **8**. Thus, in the light of the observed thermal dehydration behavior, UV/Vis, IR, and ESI-MS studies the molecular formulae of the bulk have been proposed.

Solution Studies

The structural behavior of the complexes **1**–**13** in solution has been investigated using UV/Vis, ESI-MS spectroscopic techniques.

UV/Vis Spectroscopy

Electronic spectra of the complexes **1**–**13** recorded in DMF solution and Nujol mull are shown in Table 1. The absorption bands observed in the range 620–703 nm correspond to *d-d* transitions and the strong bands at 358–402 nm are due to ligand-to-metal charge transfer. For an octahedral geometry the expected ^2E_g to $^2T_{2g}$ transition takes place at around 800 nm. This band will undergo a significant blue shift when the octahedral geometry distorts to a square pyramidal and square planar structure.[13] For the reduced Schiff base copper(II) complexes with square pyramidal geometry, the *d-d* transitions and charge transfer transitions generally occur in the range 620–720 and 360–450 nm, respectively.[8–9,14a–14d]

The medium intensity bands occurring in the range 356–401 nm are due to phenolate-to-copper(II) charge transfer.[14a–14d] As the present complexes contain the *para* substituents on the bridging phenolate, definitive assignment of CT bands can be provided based on the electronic effects induced by the substituents. Electron-donating groups are expected to decrease the Lewis acidity of the copper center thus shifting the phenoxo-to-copper CT band to lower energies while electron-withdrawing groups are expected to increase the Lewis acidity and shift the phenolate-to-copper CT bands to higher energies.[10a,14d] Accordingly, we observe the electron-donating *para* $-CH_3$ group shifting the LMCT band to lower energy and the electron-withdrawing *para* –OH and –Cl groups causing the shift of the LMCT

Table 1. Summary of the UV/Vis spectroscopic data of **1**–**13**.

Complex	Absorption bands (DMF)		(Nujol)	
	d-d (ε)[a]	CT(ε)	*d-d*	CT
$[Cu_2(Scp11)_2(H_2O)_2]$, **1**	705 (150)	380 (1780)	695	378
$[Cu_2(ClScp11)_2(H_2O)_2]$, **2**	702 (170)	356 (1340)	690	360
$[Cu_2(MeScp11)_2(H_2O)_2]$, **3**	703 (170)	394 (2050)	697	392
$[Cu_2(OHScp11)_2(H_2O)_2]$, **4**	703 (1010)	364 (1520)	696	370
$[Cu_2(Sch11)_2](H_2O)$, **5**	703 (1890)	380 (2800)	698	388
$[Cu_2(ClSch11)_2(H_2O)_2]$, **6**	704 (180)	370 (1190)	691	378
$[Cu_2(MeSch11)_2(H_2O)_2]$, **7**	702 (1860)	400 (1410)	696	398
$[\{Cu_2(Sch12)_2\}_2Cu_2(Sch12)_2(H_2O)_2]\cdot 4H_2O$, **8**	704 (530)	381 (1430)	700	382
$[Cu_2(ClSch12)_2]\cdot 2H_2O$, **9**	623 (240)	368 (1680)	628	370
$[Cu_2(MeSch12)_2(H_2O)_2]$, **10**	702 (180)	401 (2440)	697	399
$[Cu_2(Diala5)_2(H_2O)_2]\cdot H_2O$, **11**	703 (160)	364 (1740)	695	368
$[Cu_2(Diala4)_2(H_2O)_2]\cdot H_2O$, **12**	702 (210)	368 (2120)	704	364
$[Cu_2(Diala3)_2(H_2O)_2]\cdot H_2O$, **13**	703 (210)	372 (920)	702	379

[a] ($M^{-1}\,cm^{-1}$).

band to higher energy. On the basis of the crystal structure of **9a**, the geometry around the copper(II) centers in **9** is assumed to have a square-planar geometry. The observed *d-d* transitions in **9** at 623 nm also indicate square planar Cu^{II} centers. This behavior is similar to that recorded for the structurally well-characterized square planar copper(II) complexes.[13] The electronic spectra of **1**–**13** do not change much in DMF solution and Nujol mull, and appear to indicate that the coordination number and geometry observed in the solid state are retained in solution.

ESI-MS Studies

The structural behavior of the complexes **1**–**13** in solution has been investigated by ESI mass spectral analysis. ESI mass spectra of the complexes were recorded in MeOH except for **2**, **7**, and **9** for which the spectra were recorded in a 1:1 solvent mixture of MeOH and DMSO because of a solubility problem. As indicated by the masses of both positive and negative ions in the spectra, all the complexes are found to exist in solution mainly as dicopper(II) species. For example, the positive ion ESI masses observed for **8** shows the existence of dicopper(II) species predominantly in solution as $[Cu_2(Sch12)_2Na]^+$ (643, 100). The other less intense peaks found were $[Cu(Sch12)Na]^+$ (333, 27); $[Cu_3(Sch12)_3Na]^+$ (954, 55); $[Cu_4(Sch12)_4Na]^+$ (1267, 25); $[Cu_5(Sch12)_5Na]^+$ (1574, 20). Our attempts to obtain consistent electrochemical data using CV were unsuccessful owing to the solubility problem. Nonetheless, it maybe noted that the concentration levels in methanolic solutions were just enough for the activity studies.

General Description of Crystal Structures

The crystal structures of complexes **1a**, **2a**, **3a**, **4**, **6a**, **8**, **9a**, and **12a** were determined by single-crystal X-ray crystallographic analysis. In all these complexes, the reduced Schiff-base ligands display a tridentate coordination mode while bridging the two copper ions through phenolate oxygen atoms forming Cu_2O_2 cores with a Cu···Cu distance of ca. 3 Å. The crystal structure of **9a** displayed Cu^{II} centers with a square-planar geometry while the other complexes contain square pyramidal Cu^{II} centers.

In all the square pyramidal complexes, the basal plane of the square pyramid is completed by the coordination of each Cu^{II} to the two bridging phenolate oxygen atoms, imine nitrogen, and carboxylate oxygen. The Cu–O bond lengths due to the coordination of each Cu^{II} to the bridging phenolate and carboxylate oxygen atoms in the basal plane fall in the range of 1.934(2)–2.002(3) and 1.876(2)–1.982(7) Å, respectively, while the bond lengths due to Cu–N (imine nitrogen) are observed in the range of 1.950(2)–2.004(8) Å. The apical position is occupied by solvents. A crystallographic center of inversion is present in the dimeric structure of **1a**, **3a**, **4**, **6a**, and **9a**. Selected bond lengths and angles as well as hydrogen bond parameters have been compiled in Table 2 and Table 3 respectively.

With respect to the ligands, **1a**, **2a**, **3a**, and **4** contain a 1-aminocyclopentanecarboxylate side arm but different

Table 2. Selected bond lengths and bond angles for the complexes.

Complex **1a**			
Cu(1)–O(2)	1.945(2)	O(2)–Cu(1)–O(1)[a]	102.78(9)
Cu(1)–O(1)[a]	1.958(2)	O(1)–Cu(1)–Cu(1)[a]	39.44(6)
Cu(1)–O(1)	1.961(2)	N(1)–Cu(1)–Cu(1)[a]	131.92(8)
Cu(1)–N(1)	1.983(3)	C(1)–O(1)–Cu(1)[a]	133.7(2)
Cu(1)–O(4)	2.213(2)	C(1)–O(1)–Cu(1)	118.4(2)
Cu(1)–Cu(1)[a]	3.0245(7)	Cu(1)[a]–O(1)–Cu(1)	101.04(9)
Complex **2a**			
Cu(1)–O(4)	1.949(2)	O(4)–Cu(1)–N(1)	68.2(1)
Cu(1)–N(1)	1.962(3)	O(4)–Cu(1)–O(2)	102.4(1)
Cu(1)–O(2)	1.964(3)	N(1)–Cu(1)–O(2)	82.5(1)
Cu(1)–O(1)	2.002(3)	O(4)–Cu(1)–O(1)	79.2(1)
Cu(1)–O(8)	2.230(3)	N(1)–Cu(1)–O(1)	93.5(1)
Cu(1)–Cu(2)	3.0428(6)	O(2)–Cu(1)–O(1)	165.7(1)
Complex **3a**			
Cu(1)–O(2)	1.939(2)	O(2)–Cu(1)–O(1)[a]	102.02(7)
Cu(1)–O(1)[a]	1.944(2)	O(2)–Cu(1)–O(1)	174.04(7)
Cu(1)–O(1)	1.960(2)	O(1)[a]–Cu(1)–O(1)	79.33(7)
Cu(1)–N(1)	1.961(2)	O(1)[a]–Cu(1)–N(1)	171.71(7)
Cu(1)–Cu(1)[a]	3.0056(5)	O(2)–Cu(1)–Cu(1)[a]	141.57(5)
		O(1)–Cu(1)–N(1)	93.79(7)
Complex **4**			
Cu(1)–O(2)	1.920(2)	O(2)–Cu(1)–O(1)	178.97(8)
Cu(1)–O(1)	1.930(2)	O(2)–Cu(1)–O(1)[a]	102.10(8)
Cu(1)–O(1)[a]	1.934(2)	O(1)–Cu(1)–O(1)[a]	78.48(8)
Cu(1)–N(1)	1.973(2)	O(2)–Cu(1)–N(1)	84.57(9)
Cu(1)–O(4)	2.660(3)	O(1)–Cu(1)–N(1)	94.67(9)
Cu(1)–Cu(1)[a]	2.9923(7)	O(1)[a]–Cu(1)–N(1)	165.21(9)
		O(1)[a]–Cu(1)–O(4)	105.32(8)
Complex **6a**			
Cu(1)–O(2)	1.940(2)	O(2)–Cu(1)–O(1)[a]	103.62(6)
Cu(1)–O(1)[a]	1.951(1)	O(2)–Cu(1)–N(1)	83.76(7)
Cu(1)–N(1)	1.968(2)	O(1)[a]Cu(1)–N(1)	169.91(7)
Cu(1)–O(1)	1.972(1)	O(2)–Cu(1)–O(1)	173.62(6)
O(1)–Cu(1)[a]	1.951(1)	O(1)[a]–Cu(1)–O(1)	78.49(6)
Cu(1)–Cu(1)[a]	3.0382(5)	O(2)–Cu(1)–Cu(1)[a]	142.78(5)
Complex **8**			
Cu(1)–O(2)	1.91(1)	O(2)–Cu(1)–O(1)[a]	94.9(5)
Cu(1)–O(1)	1.95(1)	O(1)–Cu(1)–O(1)[a]	76.8(6)
Cu(1)–O(1)[a]	1.97(1)	O(1)[a]–Cu(1)–N(1)	154.7(6)
Cu(1)–N(1)	1.98(1)	O(1)[a]–Cu(1)–O(6)	111.8(5)
Cu(1)–O(6)	2.35(1)	O(5)–Cu(2)–O(4)[b]	96.8(5)
Cu(2)–O(5)	1.93(2)	O(4)[b]–Cu(2)–O(4)	76.1(5)
Cu(2)–O(9)	2.51(1)	O(4)[b]–Cu(2)–N(2)	161.0(6)
Cu(2)–O(4)[b]	1.96(1)	C(15)–O(4)–Cu(2)[b]	133.4(10)
O(1)–Cu(1)[a]	1.97(1)	Cu(2)[b]–O(4)–Cu(2)	103.9(5)
O(4)–Cu(2)[b]	1.96(1)	O(7)[c]–Cu(3)–O(7)	78.1(6)
Cu(3)–O(7)[c]	1.96(1)	O(7)[c]–Cu(3)–N(3)	163.4(6)
O(7)–Cu(3)[c]	1.96(1)	Cu(3)[c]–O(7)–Cu(3)	101.9(6)
Cu^{I}–Cu(1A)	3.074(4)	O(7)[c]–Cu(3)–O(11)	95.0(5)
Cu(3)–Cu(3)[c]	3.056(4)		
Complex **9a**			
Cu(1)–O(2)	1.876(2)	O(2)–Cu(1)–O(1)	164.48(9)
Cu(1)–O(1)	1.926(2)	O(2)–Cu(1)–O(1)[a]	95.72(8)
Cu(1)–O(1)[a]	1.949(2)	O(1)–Cu(1)–O(1)[a]	76.90(9)
Cu(1)–N(1)	1.950(2)	O(2)–Cu(1)–N(1)	95.98(9)
Cu(1)–Cu(1)[a]	3.0350(7)	O(1)[a]–Cu(1)–N(1)	165.17(9)
		O(2)–Cu(1)–Cu(1)[a]	132.51(6)

Table 2. *(continued)*

Complex **12a**			
Cu(1)–O(5)	1.982(7)	O(5)–Cu(1)–O(1)	102.3(3)
Cu(1)–O(1)	1.999(7)	O(5)–Cu(1)–N(2)	84.1(3)
Cu(1)–N(2)	2.004(8)	O(1)–Cu(1)–N(2)	169.1(3)
Cu(1)–O(4)	2.005(7)	O(5)–Cu(1)–O(4)	168.9(3)
Cu(1)–O(9)	2.300(7)	O(1)–Cu(1)–O(4)	77.4(3)
Cu(1)–Cu(2)	3.0225(8)	N(2)–Cu(1)–O(4)	94.7(3)
		O(5)–Cu(1)–O(9)	97.8(3)
		O(1)–Cu(1)–O(9)	93.4(3)
		N(2)–Cu(1)–O(9)	94.5(3)
		O(4)–Cu(1)O(9)	93.3(3)

[a] Symmetry transformations used to generate equivalent atoms: $-x+1, -y+1, -z+1$ (**1a**); $-x+1, -y+1, -z+1$ (**3a**); $-x+1, -y+1, -z+1$ (**4**); $-x+1, -y+1, -z+1$ (**6a**); $-x+1, -y+1, -z+1$ (**8**); $-x+1, -y+1, -z+1$ (**9a**). [b] $-x, -y, -z$ (**8**). [c] $-x+1, -y+1, -z$ (**8**).

substituents on the 5-position of the benzene ring; H in **1a**, Cl in **2a**, CH_3 in **3a**, and OH in **4a**. All these complexes, **1a**, **2a**, **3a**, and **4** display Cu^{II} centers with a distorted square pyramidal geometry (τ = 0.168, 0.043, 0.038, 0.228, and 0.003, respectively).[15] The common 1-aminocyclopentanecarboxylate side arm of the ligands in **1a**, **2a**, **3a**, and **4** resulted in the formation of five-membered rings. The complex **1a** as a methanol adduct crystallized with two methanol molecules in the monoclinic system with space group *C*2/*c* with a Cu···Cu separation of 3.0245(7) Å. The apical positions of the square pyramid of the two Cu^{II} atoms are occupied by methanol molecules in *trans* fashion (Figure 1). Complementary MeOH···O=C (O4–H4···O2) and N–H···O=C (N1–H1···O3) intermolecular hydrogen bonding generates a 1D polymeric structure in **1a** in the solid state (Figure 2).

Table 3. Hydrogen bond parameters.

D–H	*d*(D–H)	*d*(H···A)	∠DHA	*d*(D···A)	A	Symmetry
Compound **1a**						
N1–H1	0.80(3)	2.35(4)	148(4)	3.053(3)	O3	$x-1, y, z-1/2$
O4–H4	0.72(4)	1.97(4)	174(5)	2.691(4)	O2	$x-1, y, z-1/2$
Compound **2a**						
O7–H7A	0.73(6)	2.26(4)	162(6)	2.961(9)	N4S	$x+1, y, z$
O7–H7B	0.81(6)	1.92(4)	177(5)	2.728(4)	O3	$x-1, y-1, z-1$
Compound **3a**						
N1–H1	0.87(3)	2.10(3)	159(3)	2.932(3)	O5	$-x,-y+1,-z+1$
O4–H4	0.76(4)	2.05(4)	163(3)	2.785(3)	O3	$x+1, y, z$
O5–H5	0.78(6)	2.14(5)	156(5)	2.864(4)	O2	
Compound **4**						
N1–H1	0.84(3)	2.39(3)	143(3)	3.100(3)	O3	$x-1, y-1, -z$
O4–H4A	0.68(4)	2.10(4)	162(4)	2.753(3)	O3	$x-1, y-1, -z$
O4–H4B	0.75(4)	2.20(4)	146(4)	2.849(4)	O5	$x-2, -y, 1-z$
O5–H5	0.72(4)	2.05(4)	173(4)	2.770(4)	O4	$x+1, y, z$
C13–H13B	0.98	2.58	144	3.420(3)	O2	$x-1, y-1, -z$
Compound **6a**						
N1–H1	1.01(3)	1.92(3)	167(2)	2.905(3)	O5	
O4–H4	0.71(3)	2.08(3)	171(4)	2.775(2)	O3	$x-1, y, z$
O5–H5	0.75(3)	2.11(3)	169(3)	2.851(3)	O2	$-x+2, -y+1, -z+1$
Compound **8**						
N1–H1	0.81(17)	2.38(16)	157(19)	3.14(1)	O5	
N2–H2	0.8(2)	2.4(2)	164(18)	3.18(2)	O8	
N3–H3	0.85(18)	2.13(19)	170(15)	2.97(2)	O12	
O11–H11C	0.9(3)	1.9(3)	165(26)	2.83(3)	O12	
O11–H11D	0.9(2)	2.0(2)	164(27)	2.84(2)	O6	
O12–H12C	0.9(3)	1.9(3)	168(18)	2.75(2)	O2	
O13–H13C	0.9(3)	2.0(3)	153(12)	2.88(3)	O9	
O13–H13D	0.9(3)	2.02(18)	161(12)	2.89(3)	O3	
Compound **9a**						
N1–H1	0.84(4)	2.03(4)	171(3)	2.866(4)	O1S	
O1S–H1S	0.79(4)	1.89(4)	166(5)	2.667(4)	O3	$-x+1, -y+1, -z$
Compound **12a**						
N1–H1	0.92	2.11	153	2.96(1)	O11	
N2–H2	0.92	2.08	146	2.89(1)	O12	
O7–H7	0.83	1.87	164	2.68(1)	O3	$x+1, y+1, z$
O8–H8A	0.83	1.93	154	2.70(1)	O6	$x-1, y-1, z$

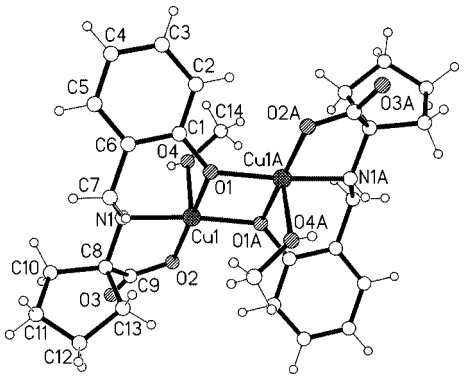

Figure 1. A perspective view of the dimer **1a** (symmetry equivalent positions: $-x+1$, $-y+1$, $-z+1$).

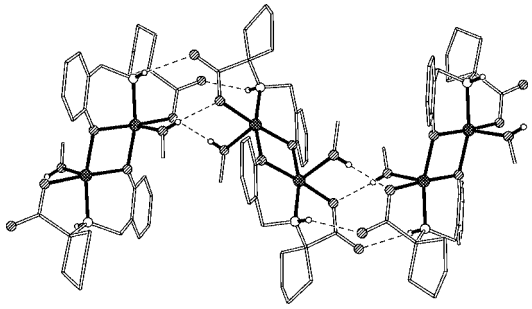

Figure 2. A view showing a portion of the 1D hydrogen-bonded structure in **1a**.

In **2a** the two copper atoms in the dimer are separated by a distance of 3.0428(6) Å. The apical site of the square pyramid is occupied by DMF [Cu(1)–O(8), 2.230(3) Å] with Cu(1) and the aqua ligand [Cu(2)–O(7), 2.299(3) Å] with Cu(2) in *trans* to each other. Each dimer is associated with two molecules of acetonitrile solvent in the asymmetric unit. There are very weak interactions between the carbonyl oxygen atoms and the copper atoms [Cu(1)···O3(1 – *x*, 1 – *y*, 1 – *z*), 2.885 Å and Cu(2)···O6(1 – *x*, *y*, *z*), 2.922 Å] that are about the sum of the van der Waals radii, 2.9 Å. These Cu···O interactions generate a 1D polymer along the *b*-axis sustained by hydrogen bonds between carboxylate oxygen and the aqua ligand, O(7) H(7B)···O(3). Further O(7)–H(7A)···N(4S) hydrogen bonds have also been observed.

The complex **3a** displays square pyramidal geometry at each Cu^{II} center with a Cu···Cu distance of 3.0056(5) Å. The apical sites of the square pyramid at each Cu^{II} center are occupied by methanol molecules in *trans* fashion with a Cu···O distance of 2.59 Å. Packing of dimers along the *a* axis displays a 1D hydrogen-bonded polymer in **3a** supported by intermolecular hydrogen bonds generated between imine H atoms and methanol oxygen [N–H···O(5)], methanolic hydrogen, and carboxylate oxygen atoms [O(4)–H(4)···O(3) and O(5)–H(5)···O(2)] as well as weak interactions of neighboring carboxylate oxygen atoms with each Cu^{II} ion (Cu···O, 2.885 Å) in *syn-anti* fashion.

In the crystal structure of **4** the two lattice water molecules are in close interaction with Cu^{II} atoms [Cu–O, 2.66(3) Å] occupying the apical positions to complete the square pyramidal geometry around each Cu^{II} center (Figure 3) with a Cu···Cu distance of 2.9924(8) Å. Intermolecular hydrogen bonds generated by the hydroxy group on the phenolate moiety with the aqua ligand (O4–H4B···O5, O5–H5···O4) and carboxylate oxygen atom (O4–H4A···O3) and by the imine hydrogen with another carboxylate oxygen (N1–H1···O3) have resulted in a 3D hydrogen-bonded network in **4** as shown in Figure 4.

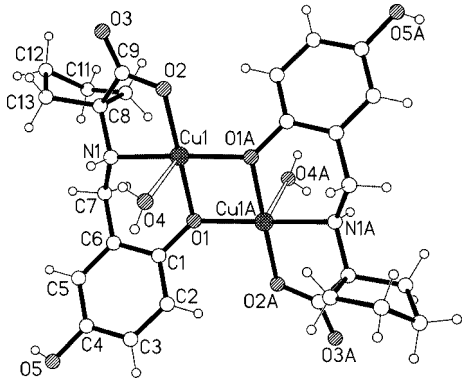

Figure 3. A perspective view of the dimer **4** (symmetry equivalent positions: $-x+1$, $-y+1$, $-z+1$).

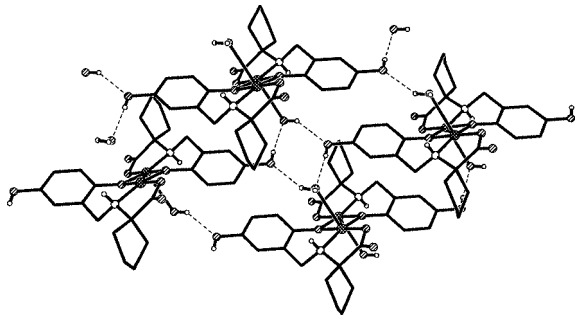

Figure 4. Packing diagram of **4**.

The compound **6** crystallized in triclinic space group $P\bar{1}$ with two methanol molecules in the crystal lattice and **6a** is isomorphous to **3a**, i.e. the arrangement of molecules in the crystal lattice, but not isostructural. The hydrogen bonding pattern in **6a** is also similar to that observed in **3a**. The solid-state crystal packing along the *b* axis revealed that the complex is a 1D polymer that resulted from weak Cu···O interactions and intermolecular hydrogen bonding. Further, carboxylate oxygen atoms of the neighboring dimeric units maintain weak interactions with each Cu^{II} ion (Cu···O, 2.95 Å) in *syn-anti* mode. In addition to these interactions, crystal packing also reveals that N–H hydrogen atoms are involved in the intermolecular hydrogen bonding to methanolic oxygen atoms [N(1)–H(1)···O(5)] and the methanolic hydrogen atoms maintain intermolecular hydrogen bonds to carboxylate oxygen atoms [O(4)–H(4)···O(3) and O(5)–H(5)···O(2)].

In the crystal structure of **8** for $Z = 3$ in the triclinic space group $P\bar{1}$, there are three independent Cu^{II}–Sch12 units and each one is near an inversion center (1/2, 1/2, 1/2), (0,0,0), and (1/2, 1/2, 0) as illustrated in Figure 5. Of

these Cu3 has an aqua ligand in the apical position. The O9 of the carboxylate group from this unit is bonded to Cu2 with the Cu2–O9 distance of 2.51(1) Å. Similarly, O6 occupies the apical axial position of the Cu1 [Cu1–O6, 2.36(1) Å] with a distorted square pyramidal geometry. On the other hand, the oxygen atom of the third carboxylate group, O3, is only involved in hydrogen bonding to a hydrogen atom, H13D of lattice water. The axial bonding of the carbonyl oxygen atoms O6 and O9 from neighboring dimeric units to Cu1 and Cu2 centers produces a 2D coordination polymeric structure and the interdimer connectivity leads to the formation of a 2D (4, 4) network structure as shown in Figure 6 and these (4, 4) nets are well known in coordination polymeric structures.[16]

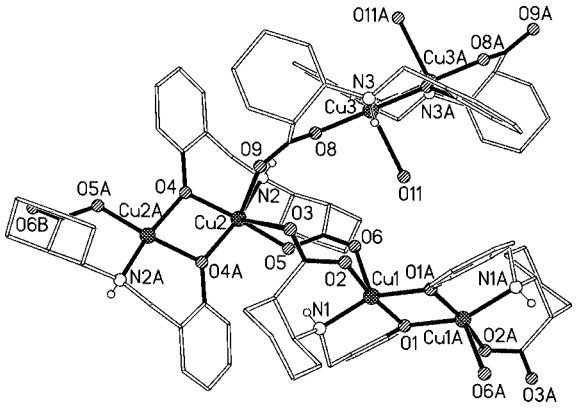

Figure 5. Perspective view of the unit cell contents in **8**. The lattice water molecules are omitted for clarity.

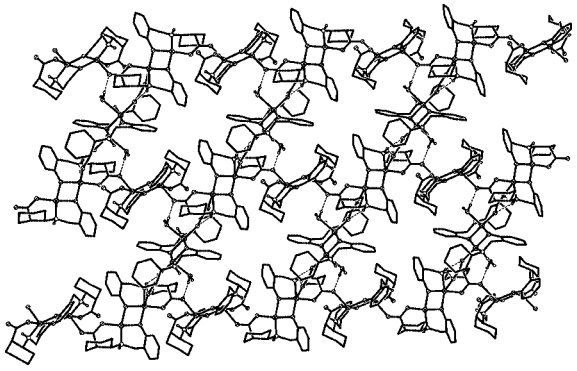

Figure 6. Portion of packing diagram of **8** showing the 2D connectivity. The hydrogen atoms and lattice water molecules have been omitted for clarity.

In this series, the only compound that displays a square-planar geometry at the Cu^{II} atoms is **9a**. The unit cell contains two methanol molecules involved in hydrogen bonding via imine nitrogen [N(1)–H(1)···O(1S)] and carboxylate oxygen [O(1S)–H(1S)···O(3)], which lead to the formation of a 1D polymeric structure. The hydrogen bond lengths observed in the solid-state packing of **9a** are found to vary between 1.90 and 2.38 Å. Table 3 contains selected hydrogen bond parameters. These hydrogen bonds are considered to be normal as compared to the available literature on N–H···O and O–H···O hydrogen bond parameters.[17]

The dimer **12a** crystallized with four DMSO molecules of which two are bonded at the apical positions of each Cu^{II} in the dimer and two are hydrogen-bonded to the imine hydrogen atoms through N–H···O interactions. The two DMSO molecules are disposed in *anti* fashion probably due to the bulkiness of the axial substitution. This causes the dimer to have a pseudo-center of inversion which is unprecedented in these types of structure having chiral reduced Schiff-base ligands.[6] A ribbon-like 1D hydrogen-bonded polymeric structure is produced by complementary O–H···O bonds between phenolic hydrogen and oxygen atoms of the carboxylate group. All these polymers are aligned parallel to the (1$\bar{1}$0) plane. Acetone molecules filled the empty cavities between these strands.

Magnetic Studies of $[\{Cu_2(Sch12)_2\}_2Cu_2(Sch12)_2(H_2O)_2]\cdot 4H_2O$ (8)

It is evident from the previous section that only complexes **4** and **8** furnished the single crystals that represent the structures of the bulk. Further, the inter-dimer connectivity in **8** generated an interesting 2D (4, 4) coordination polymeric network structure. Hence, we investigated the variable temperature magnetic moments for **8** in order to understand the inter-dimer magnetic coupling interactions mediated by *syn-anti* carboxylate bridging.

The temperature dependences of χ_m and $\chi_m T$ for crystalline samples of **8** per Cu_2 unit are presented in Figure 7. On lowering the temperature, χ_m decreases gradually, there is an increase below ca. 70 K; while the $\chi_m T$ value even at 330 K (0.383 $cm^3 mol^{-1} K$) is quite small compared with the expected value 0.75 $cm^3 mol^{-1} K$ for two noninteracting Cu^{II} ions, upon cooling it decreases rapidly to a value close to zero at 2 K. The increase of χ_m at low temperature should be due to trace paramagnetic impurity (ρ). Overall, the data suggest a strong antiferromagnetic coupling between the adjacent Cu ions in **8**. The coupling between the dinuclear moiety in the 2D layer of **8** is negligible, as expected, because of both the *syn-anti* carboxylate bridging

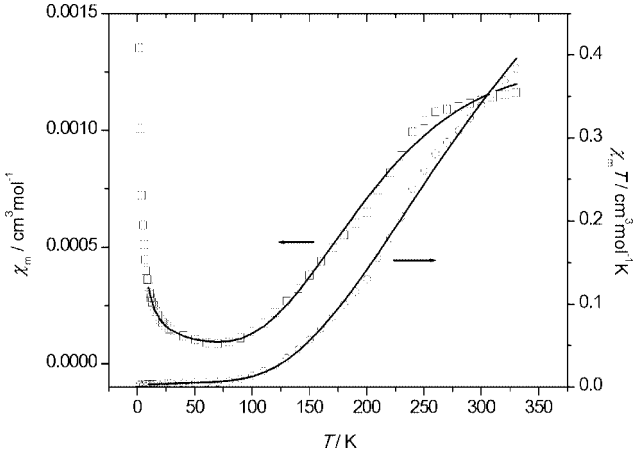

Figure 7. The temperature dependences of χ_m and $\chi_m T$ in the range of 2–350 K for **8**. The solid lines represent the fit using a Cu_2 dimer model.

mode and the orthogonal relationship of the planes of the neighboring Cu_2O_2.[14b] Therefore, the magnetic data of **8** can be analyzed by fitting the susceptibilities to an equation calculated using an $H = -2JS_1S_2$ Hamiltonian for a dimer plus impurity of the monomer model.[14e–14f] The parameters have their usual meanings. As shown in Figure 7, a reasonable fit was obtained with the results: $J = -230(3)\ cm^{-1}$, $g = 2.29(2)$, $\rho = 0.0056$; $N_\alpha = 4.9\times10^{-6}$ with $R = 1.4\times10^{-3}$ $\{R = \sum[(\chi_m)_{obs} - (\chi_m)_{calc}]^2/\sum[(\chi_m)_{obs}]^2\}$.

Catecholase Biomimetic Studies

In order to gain deeper insight into the various parameters that determine the copper-mediated substrate oxidations and bimetallic reactivity both in natural metalloenzymes and in synthetic analogues, quite a number of mono- and dinuclear copper(II) complexes have been investigated as biomimetic catalysts for catechol oxidation.[18–23] In all these investigations, a common and convenient model substrate, 3,5-DTBC was used due to its low redox potentials.[20] Some of the crucial factors dictating the catecholase activity can now be highlighted based on many investigations correlating various structural parameters of the dicopper(II) complexes with their activity; viz., the distance between the Cu^{II} centers,[24] the nature of the bridging group between the copper ions,[25] electronic properties of the complexes,[10,26] and the geometric changes of the dicopper core.[27] Furthermore, the factors such as the number of donor sites, nature of the donors, and the rigidity of the ligand or the bridging moiety imposing strain in the complex have also been found to play a vital role.[28] However, the studies correlating the activity with electronic effects due to substituents on the bridging phenolate have not been well explored.[10] Since the present series of complexes contain both electron-donating and -withdrawing substituents on the phenyl ring we have attempted to investigate their activity.

On the basis of the chemical and spectroscopic characterizations of the complexes **1**–**13** and the crystal structures of selected compounds, all these complexes are characterized by active Cu_2O_2 centers with a Cu···Cu distance of ca. 3 Å, which is favorable for the efficient binding of the substrate. Minor changes observed in the UV/Vis spectra recorded in DMF solution compared to Nujol mull indicate that the coordination number and geometry of **1**–**13** are retained in solution. Further, ESI-MS studies confirm the existence of copper(II) dimers in solution. Subsequently, all the complexes exhibit significant activity due to the presence of active dicopper(II) cores. The course of oxidation of 3,5-DTBC catalyzed by **8** is shown in Figure 8. The kinetic parameters have been determined by applying the Michaelis–Menten approach. A linear relationship for the initial rates and the concentration of the complexes has been obtained for **1**–**13**, which shows a first-order dependence of the rate on the catalyst concentration. An example of a Lineweaver–Burk plot[18f] is given in Figure 9 for **8**. Kinetic parameters of the complexes are given in Table 4.

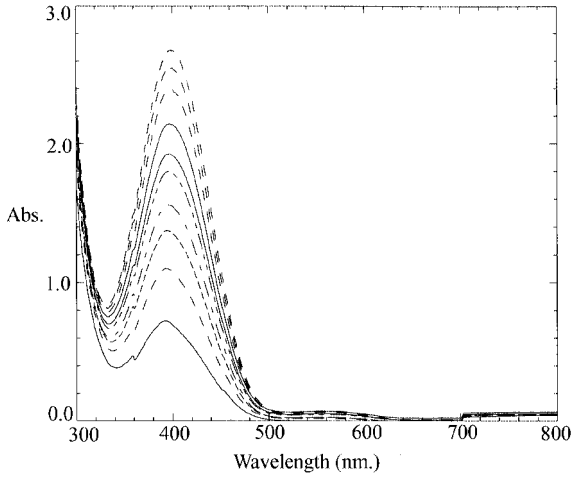

Figure 8. Oxidation of 3,5-DTBC by **8** monitored by UV/Vis spectroscopy. Higher concentrations were used only to emphasize the bands for the oxidation process.

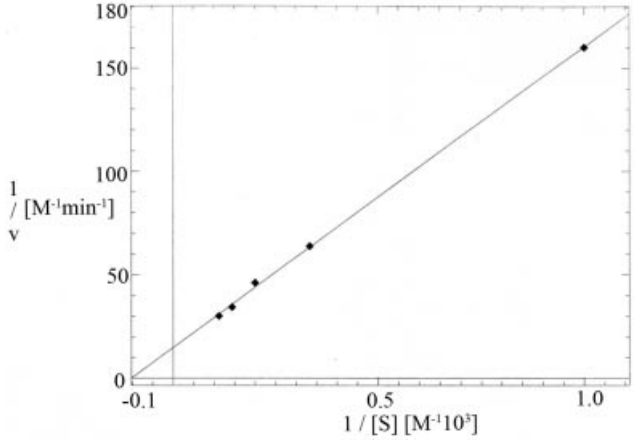

Figure 9. Lineweaver–Burk plot for the catalysis by **8**.

Table 4. Kinetic parameters for the oxidation of 3,5-DTBC by the complexes **1**–**13**.[a]

Complex	Substituent (R)	K_{cat} [h^{-1}]	K_m [mM]	V_{max} [$10^6\ Ms^{-1}$]
1	–H	850(28)	22.3(4)	30.2(6)
2	–Cl	694(32)	26.2(3)	22.4(1)
3	$-CH_3$	1003(59)	15.4(6)	34.3(6)
4	–OH	773(30)	20.6(7)	26.7(3)
5	–H	863(28)	18.5(5)	30.2(1)
6	–Cl	785(49)	20.3(8)	24.5(5)
7	$-CH_3$	1080(30)	14.6(3)	36.1(2)
8	–H	2006(44)	9.2(1)	68.5(4)
9	–Cl	883(33)	17.7(3)	29.3(3)
10	$-CH_3$	3120(28)	4.3(1)	104.6(6)
11	*para* –OH	595(27)	21.4(4)	22.3(7)
12	*meta* –OH	513(21)	28.6(4)	19.4(8)
13	*ortho* –OH	460(14)	31.3(3)	17.6(5)

[a] The values were obtained from three measurements.

It is obvious from Table 4 that the activity of **1**–**4** follows the order **3** > **1** > **4** > **2** with **3** showing higher activity (K_{cat} = 1003 h^{-1}). Further, the activity of **2** has noticeably

decreased due to the strong electron-withdrawing nature of *Cl* when compared to the activity of **4** containing the *–OH* group.[29] Thus, with respect to the substituents on the bridging phenolate, the activity of the corresponding complexes followed the order: $CH_3 > H > OH > Cl$. A similar trend (**7** > **5** > **6**) has been observed (Table 4) for Cu^{II} complexes of RSch11 ligands, **5**–**7**. Among **8**–**10**, the *methyl*-substituted **10** exhibited significantly higher activity (K_{cat} = 3120 h^{-1}) while *chloro*-substituted **9** with Cu^{II} in a square-planar geometry showed a lower activity (K_{cat} = 883 h^{-1}) following a similar trend. Earlier investigations on the activity of copper(II) systems have shown that the square planar copper(II) complexes are weak catechol-oxidase catalysts.[19,22,24d,28,31] However, reports are also available on square planar dicopper(II) complexes showing very high activity.[18f,25] On the same grounds, **9** with a similar geometry exhibiting significant activity can be another example for the latter.

The six-membered chelate rings facilitate strain-free substrate binding compared to the five-membered rings[9,18f,28] by offering a flexible and relaxed coordination sphere at Cu^{II} centers thus enhancing the activity of **8** compared to the activities of **1** (K_{cat} = 850 h^{-1}), and **5** (K_{cat} = 863 h^{-1}) forming five-membered rings. Furthermore, it is also the formation of six-membered rings that significantly enhanced the activity of **10** (K_{cat} = 3120 h^{-1}) compared to **3** (K_{cat} = 1003 h^{-1}) or **7** (K_{cat} = 1080 h^{-1}) which contain five-membered rings. It may be noted that these complexes (**3**, **7**, and **10**) have *para* methyl phenyl rings.

In the case of **11**–**13** containing Diala ligands, the trend in K_{cat} is **11** > **12** > **13** (Table 4). The activity of **11** (K_{cat} = 595 h^{-1}) with a *para*-hydroxy bridging phenolate is found to be higher than that of **12** (K_{cat} = 513 h^{-1}) and **13** (K_{cat} = 460 h^{-1}) containing *meta*- and *ortho*-hydroxy bridging phenolate moieties, respectively. These variations in the activity maybe attributed to the differences in the steric match[18,27,28] caused by the respective changes in the position of the *–OH* group on the bridging phenolate. Further, comparing the activity (K_{cat} = 666 h^{-1}), under similar experimental conditions, of our previously reported unsubstituted complex $[Cu_2(L\text{-}Sala)_2(H_2O)]$[8] with the activity ($K_{cat}$ = 595 h^{-1}) of the present *para* hydroxy-substituted **11** it is obvious that the decrease in the activity of **11** can be attributed to the effect of the electron-withdrawing *-OH* group on the phenyl ring of the ligand.

The kinetic data for **1**–**13** presented in Table 4 shows that the substitution of phenolate by electron-donating substituents increased the activity while the substitution by electron-withdrawing groups decreased the activity. In the absence of electrochemical data for **1**–**13**, it is difficult to conclude that the catalytic efficiency is solely governed by the electronic influence of the substituents except envisaging a rough correlation. Moreover, no clear and direct correlation has been established so far between the rates of reaction, redox potentials, and electronic effects of the complexes.[10,26,28] However, other factors such as geometry, steric factors, and interactions between the substrate and catalyst can also influence the overall efficiency. It should also be noted that the exact Cu···Cu separation in solid-state structures need not be retained in the solution, and direct correlation between the Cu···Cu distance and catalytic activity need not be expected. However, based on the information regarding the geometries and molecular species obtained from the solution studies involving the techniques such as UV/Vis spectroscopy and ESI-MS at least some correlations can be achieved.

Recently, Wegner et al. reported the most active catalyst among the known functional model complexes so far, with a turnover number or K_{cat} of 9927 h^{-1}.[5h] When compared mainly with the turnover numbers of 1188 h^{-1}, 2804 h^{-1}, and 5470 h^{-1}, reported by Monzani et al.,[31–32] Meyer et al., [27] and Mukherjee et al.[25a] respectively, and with the other lower to moderate turnover values,[5,10,18–19,22–30] the observed turnover rates of 460 to 3120 h^{-1} may suggest moderate to high catalytic activity of the present complexes. However, all activity studies on the model complexes synthesized so far have only achieved turnover numbers of about several thousand-fold lower when compared to the turnover number of native enzymes[31,26a] (for example catechol oxidase from sweet potatoes has been found to be highly active with a K_{cat} of 2293 s^{-1} especially towards catechol).[33] The current high activity in **10** (K_{cat} = 3120 h^{-1}) observed among the present model catalysts has been found to be ca. 2600-fold slower towards the oxidation of 3,5-DTBC when compared to the natural enzyme. Finally, these findings suggest that significant differences in the catalytic ability of dicopper(II) complexes can be induced by the judicious choice of different sets of binucleating ligands.

Summary

A new series of dicopper(II) complexes **1**–**13** containing reduced Schiff-base ligands formed between different substituted salicylaldehydes and amino acids have been synthesized and characterized by physicochemical and spectroscopic methods. On the basis of the single-crystal X-ray crystallographic studies of selected compounds, it can be suggested that all the complexes contain Cu_2O_2 cores with a Cu···Cu distance of ca. 3 Å. In view of the interesting 2D coordination polymeric structure, variable temperature magnetic studies carried out on **8** suggested the presence of strong intradimer antiferromagnetic coupling.

The catecholase activity of the complexes **1**–**4**, **5**–**7**, **8**–**10**, and **11**–**13** containing 1-aminocyclopentane-1-carboxylate, 1-aminocyclohexane-1-carboxylate, 2-aminocyclohexane-1-carboxylate, and L-alanine side chains, respectively, in the corresponding reduced Schiff-base ligands has been evaluated and systematically compared. It has been found that the presence of electron-withdrawing groups decreased the activity while the electron-donating groups enhanced the activity of the complexes. Under similar experimental conditions the activity shown by the current series of dicopper(II) complexes can be considered moderate to high as observed in our previous results.[8–9]

Experimental Section

Materials and Physical Measurements

All the chemicals were purchased from commercial sources and used as received for syntheses. All the solvents used were of reagent grade. The yields are reported with respect to the metal salts.

The ^{1}H NMR spectra were recorded with a Bruker ACF 300FT-NMR spectrometer using TMS as an internal reference at 25 °C and the infrared spectra (KBr pellet) were recorded using a FTS 165 Bio-Rad FTIR spectrometer in the range 4000–400 cm^{-1}. The electronic transmittance spectra were recorded with a Shimadzu UV-2501/PC UV/Vis spectrometer in DMF and Nujol mull. ESI-MS spectra were recorded using a Finnigan MAT LCQ Mass Spectrometer using the syringe-pump method. The elemental analyses were performed in the Micro Analytical Laboratory, Department of Chemistry, National University of Singapore. Water present in the compounds was determined using a SDT 2960 TGA Thermal Analyzer with a heating rate of 10 °C min^{-1} using a sample size of 7–10 mg per sample run. Room-temperature magnetic susceptibility measurements were carried out with a Johnson–Mathey Magnetic Susceptibility balance with Hg[Co(SCN)$_4$] as the standard. Variable temperature magnetic studies were made using a Quantum Design MPMS-XL5 SQUID magnetometer operating in an applied field of 5 kOe. Corrections for diamagnetism were made using Pascal's constants. Optical rotation was measured on the specified solutions in a 0.1-dm cell at 27 °C using a Perkin–Elmer model 341 polarimeter. The concentration of the solutions was 5.5 mg mL^{-1} for both the ligands (in MeOH) and complexes (in DMSO). The optical rotation of the ligands was recorded at the wavelength of 365 nm where as for the complexes the measurements were conducted at the wavelength of the D line (578 nm) of sodium.

Ligands

All the ligands except H_3Diala5, H_3Diala4, and H_3Diala3 have been synthesized using the same molar quantities according to the procedure described for H_2Scp11 in our earlier report.[6c]

1-[(5-Chloro-2-hydroxybenzyl)amino]cyclopentane-1-carboxylic Acid (H_2ClScp11): This compound was prepared from 1-aminocyclopentane-1-carboxylic acid and 5-chlorosalicylaldehyde. Yield: 0.92 g (73%). m.p. 271–272 °C. $C_{13}H_{16}ClNO_3$ (269.7): calcd. C 57.8, H 5.9, N 5.2; found C 57.2, H 6.0, N 5.7. IR (KBr): $\tilde{\nu}$ = 2966 m (NH), 1566 s υ_{as}(COO$^-$), 1384 s υ_s(COO$^-$), 1276 s (phenolic CO) cm^{-1}. ^{1}H NMR (CD$_3$OD): δ = 1.83–2.28 (m, 8 H, -C$_5$H$_8$), 4.12 (s, 2 H, benzylic), 6.83–7.36 (m, 3 H, Ar-H). ^{13}C NMR (CD$_3$OD): δ = 25.9, 37.3, 47.5, 48.1, and 48.4 (-C$_5$H$_8$), 72.9 (benzylic), 119.4, 122.3, 127.4, 129.1, 129.5, and 160.6 (aromatic), 182.7 (-COOH). EI-MS: *m*/*z* (%) = 269.2.

1-[(2-Hydroxy-5-methylbenzyl)amino]cyclopentane-1-carboxylic Acid (H_2MeScp11): This compound was prepared from 1-aminocyclopentane-1-carboxylic acid and 5-methylsalicylaldehyde. Yield: 0.92 g (76%). m.p. 272–273 °C. $C_{14}H_{19}NO_3$ (249.3): calcd. C 67.4, H 7.6, N 5.6; found C 67.0, H 7.7, N 5.9. IR (KBr): $\tilde{\nu}$ = 3447 m (OH), 2956 m (NH), 1571 s υ_{as}(COO$^-$), 1383 s υ_s(COO$^-$), 1277 s (phenolic CO) cm^{-1}. ^{1}H NMR (CD$_3$OD): δ = 1.89–2.11 (m, 8 H, -C$_5$H$_8$), 2.35 (s, Ar–CH$_3$), 3.62 (s, 2 H, benzylic), 6.53–6.83 (m, 3 H, Ar-H). ^{13}C NMR (CD$_3$OD): δ = 20.6 (Ar–CH$_3$), 24.3, 26.1, 37.6, 47.4, and 48.2 (-C$_5$H$_8$), 72.8 (benzylic), 118.4, 126.0, 127.1, 129.6, 130.6, and 160.3 (aromatic), 184.0 (-COOH). ESI-MS: *m*/*z* (%) = 249.2.

1-[(2,5-Dihydroxybenzyl)amino]cyclopentane-1-carboxylic Acid (H_2(OH)Scp11): This compound was prepared from 1-aminocyclopentane-1-carboxylic acid and 5-hydroxysalicylaldehyde. Yield: 0.75 g (63%). m.p. 263–264 °C. $C_{13}H_{17}NO_4$ (251.6): calcd. C 62.1, H 6.8, N 5.5; found C 62.0, H 6.9, N 5.6. IR (KBr): $\tilde{\nu}$ = 3398 m (OH), 2960 m (NH), 1582 s υ_{as}(COO$^-$), 1390 s υ_s(COO$^-$), 1276 s (phenolic CO) cm^{-1}. ^{1}H NMR (CD$_3$OD): δ = 1.73–2.11 (m, 8 H, -C$_5$H$_8$), 3.83 (s, 2 H, benzylic), 6.43–6.51 (m, 3 H, Ar-H). ^{13}C NMR (CD$_3$OD): δ = 24.7, 26.1, 36.0, 37.6, and 40.9 (-C$_5$H$_8$), 72.7 (benzylic), 117.6, 118.7, 119.6, 126.3, 148.2, and 159.6 (aromatic), 184.1 (-COOH). ESI-MS: *m*/*z* (%) = 251.

1-[(2-Hydroxybenzyl)amino]cyclohexane-1-carboxylic Acid (H_2Sch11): This compound was prepared from 1-aminocyclohexane-1-carboxylic acid and salicylaldehyde. Yield: 1.06 g (90%). m.p. 296–297 °C. $C_{14}H_{19}NO_3$ (249.3): calcd. C 67.4, H 7.6, N 5.6; found C 67.4, H 7.7, N 5.5. IR (KBr): $\tilde{\nu}$ = 2941 m (NH), 1577 s υ_{as}(COO$^-$), 1388 s υ_s(COO$^-$), 1272 s (phenolic CO) cm^{-1}. ^{1}H NMR (CD$_3$OD): δ = 1.43–2.03 (m, 10 H, -C$_6$H$_{10}$), 3.70 (s, 2 H, benzylic), 6.41–7.02 (m, 4 H, Ar-H). ^{13}C NMR (CD$_3$OD): δ = 23.0, 27.0, 34.5, 37.1, 48.1, and 48.4 (-C$_6$H$_{10}$), 64.3 (benzylic), 117.7, 118.3, 127.0, 129.3, 130.0, and 162.5 (aromatic), 182.8 (-COOH). ESI-MS: *m*/*z* (%) = 249.2

1-[(5-Chloro-2-hydroxybenzyl)amino]cyclohexane-1-carboxylic Acid (H_2ClSch11): This compound was prepared from 1-aminocyclohexane-1-carboxylic acid and 5-chlorosalicylaldehyde. Yield: 0.88 g (66%). m.p. 290–291 °C. $C_{14}H_{18}ClNO_3$ (283.7): calcd. C 59.3, H 6.4, N 4.9; found C 59.0, H 6.5, N 4.9. IR (KBr): $\tilde{\nu}$ = 3462 m (OH), 2940 m (N–H), 1568 s υ_{as}(COO$^-$), 1495 s υ_s(COO$^-$), 1273 s (phenolic CO) cm^{-1}. ^{1}H NMR (CD$_3$OD): δ = 1.41–2.03 (m, 10 H, -C$_6$H$_{10}$), 3.70 (s, 2 H, benzylic), 6.60–7.01 (m, 4 H, Ar-H). ^{13}C NMR (CD$_3$OD): δ = 23.4, 26.9, 34.3, 37.0, 46.1, and 48.2, (-C$_6$H$_{10}$), 64.61 (benzylic), 119.6, 121.7, 128.2, 128.9, 129.4, and 161.5 (aromatic), 182.2 (-COOH). ESI-MS: *m*/*z* (%) = 283.7.

1-[(2-Hydroxy-5-methylbenzyl)amino]cyclohexane-1-carboxylic Acid (H_2MeSch11): This compound was prepared from 1-aminocyclohexane-1-carboxylic acid and 5-methylsalicylaldehyde. Yield: 0.81 g (66%). m.p. 295–296 °C. $C_{15}H_{21}NO_3$ (263.3): calcd. C 68.4, H 8.0, N 5.3; found C 67.9, H 8.0, N 5.4. IR (KBr): $\tilde{\nu}$ = 3450 m (OH), 2932 m (NH), 1624 s υ_{as}(COO$^-$), 1381 s υ_s(COO$^-$), 1262 s (phenolic CO) cm^{-1}. ^{1}H NMR (CD$_3$OD): δ = 1.40–2.17 (m, 10 H, -C$_6$H$_{10}$), 2.38 (CH$_3$), 3.71 (s, 2 H, benzylic), 6.60–6.88 (m, 4 H, Ar-H). ^{13}C NMR (CD$_3$OD): δ = 20.5 (Ar–CH$_3$), 23.3, 26.8, 34.3, 37.0, 47.2, and 48.2, (-C$_6$H$_{10}$), 64.4 (benzylic), 117.0, 125.3, 128.8, 129.7, 130.3, and 156.8 (aromatic), 182.71 (-COOH). ESI-MS: *m*/*z* (%) = 263.3.

2-[(2-Hydroxybenzyl)amino]cyclohexane-1-carboxylic Acid (H_2Sch12): This compound was prepared from 2-aminocyclohexanecarboxylic acid and salicylaldehyde. Yield: 1.05 g (89%). m.p. 238–239 °C. $C_{14}H_{19}NO_3$ (249.3): calcd. C 67.4, H 7.7, N 5.6; found C 67.0, H 7.6, N 5.5. IR (KBr): $\tilde{\nu}$ = 2853 m (N–H), 1580 s υ_{as}(COO$^-$), 1461 s υ_s(COO$^-$), 1263 s (phenolic CO) cm^{-1}. ^{1}H NMR (CD$_3$OD): δ = 1.38–2.07 (m, 8 H, -C$_6$H$_{10}$), 2.62 (t, 1 H, HC–N), 3.01 (t, 1 H, HC–COO$^-$), 4.06 (s, 2 H, benzylic), 6.53–7.05 (m, 4 H, Ar-H). ^{13}C NMR (CD$_3$OD): δ = 24.0, 25.1, 28.2, 29.2, 48.1, and 48.4 (-C$_6$H$_{10}$), 57.4 (benzylic), 116.4, 119.1, 125.8, 129.4, 129.6, and 164.5 (aromatic), 182.3 (-COOH). ESI-MS: *m*/*z* (%) = 249.3.

2-[(5-Chloro-2-hydroxybenzyl)amino]cyclohexane-1-carboxylic Acid (H_2ClSch12): This compound was prepared from 2-aminocyclohexanecarboxylic acid and 5-chlorosalicylaldehyde. Yield: 0.18 g (64%). m.p. 233–234 °C. $C_{14}H_{18}ClNO_3$ (283.7): calcd. C 59.3, H 6.4, N 4.9; found C 59.1, H 6.4, N 4.8. IR (KBr): $\tilde{\nu}$ = 2940 m (NH), 1579 s υ_{as}(COO$^-$), 1449 s υ_s(COO$^-$), 1268 s (phenolic CO) cm^{-1}. ^{1}H NMR (CD$_3$OD): δ = 1.34–2.10 (m, 8 H, -C$_6$H$_{10}$), 2.61 (t, 1 H, HC–N), 2.98 (t, 1 H, HC–COO$^-$), 3.96 (s, 2 H, benzylic), 6.54–7.01 (m,

3 H, Ar-H). ^{13}C NMR (CD_3OD): δ = 21.4, 22.2, 25.5, 26.3, 44.5, and 45.4 (-C_6H_{10}), 55.3 (benzylic), 117.0, 117.4, 117.7, 124.4, 126.3, and 161.5 (aromatic), 179.2 (-COOH). ESI-MS: *m*/*z* (%) = 283.3.

2-[(2-Hydroxy-5-methylbenzyl)amino]cyclohexane-1-carboxylic Acid (H_2MeSch12): This compound was prepared from 2-aminocyclohexanecarboxylic acid and 5-methylsalicylaldehyde. Yield: 60%. m.p. 285–286 °C. $C_{15}H_{21}NO_3$ (263.3): calcd. C 68.4, H 8.0, N 5.3; found C 68.1, H 8.0, N 5.0. IR (KBr): $\tilde{\nu}$ = 2941 m (N–H), 1632 s $\upsilon_{as}(COO^-)$, 1459 s $\upsilon_s(COO^-)$, 1272 s (phenolic CO) cm^{-1}. ^{1}H NMR (CD_3OD): δ = 1.34–2.17 (m, 8 H, -C_6H_{10}), 2.37 (Ar–CH_3), 2.57 (t, 1 H, HC–N), 2.97 (t, 1 H, HC–COO^-), 3.96 (s, 2 H, benzylic), 6.55–6.87 (m, 3 H, aromatic). ^{13}C NMR (CD_3OD): δ = 20.5 (CH_3), 25.1, 28.0, 29.1, 37.0, 47.1, and 48.4 (-C_6H_{10}), 57.1 (benzylic), 117.4, 117.8, 123.4, 127.4, 130.2, and 159.3 (aromatic), 182.0 (-COOH). ESI-MS: *m*/*z* (%) = 263.4.

The ligands H_3Diala5, H_3Diala4, and H_3Diala3 were synthesized as described below.

***N*-(2,5-Dihydroxybenzyl)-L-alanine (H_3Diala5):** A mixture of L-alanine (0.9 g, 10.1 mmol) and NaOH (0.4 g, 10.1 mmol) in methanol (20 mL) was stirred for 20 min to get a clear solution. To this was added 2,5-dihydroxybenzaldehyde (1.4 g, 10.1 mmol). After stirring for 1 h, the resulting yellow solution was cooled in an ice bath and then treated with $NaBH_4$ (0.42 g, 11.11 mmol). The yellow color slowly disappeared. After 45 min, the pH of the solution was brought to 5 by adding acetic acid. Upon stirring for 40 min, a pale-brown solid separated out. Filtration followed by washing with methanol (2 × 5 mL), diethyl ether (2 × 5 mL), and then drying under vacuum afforded pure H_3Diala5. Yield: 1.82 g (85%). m.p. 268–270 °C. $C_{10}H_{13}NO_4$ (211.2): calcd. C 56.8, H 6.2, N 6.6; found C 56.3, H 6.3, N 6.5. IR (KBr): $\tilde{\nu}$ = 3438 m (OH), 2487 m (NH), 1635 s $\upsilon_{as}(COO^-)$, 1511 s $\upsilon_s(COO^-)$, 1285 s (phenolic CO) cm^{-1}. ^{1}H NMR ([D$_6$]DMSO): δ = 1.31 (m, 3 H, CH_3), 3.21 (m, 1 H, -CH), 3.92 (m, 2 H, benzylic), 6.61–6.72 (m, 3 H, Ar-H). ^{13}C NMR: δ = 15.7 ($CHCH_3$), 45.5 (benzylic), 56.2 (-$CHCH_3$), 116.0, 116.2, 116.9, 120.3, 148.6, and 149.6 (aromatic), 171.3 (-COOH). ESI-MS: *m*/*z* (%) = 211.4. $[\alpha]_D^{27}$: 7.4 (*c* = 5.5 mg mL^{-1}, MeOH).

***N*-(2,4-Dihydroxybenzyl)-L-alanine (H_3Diala4):** This ligand was synthesized according to the same procedure as H_3Diala4 except that 2,4-dihydroxybenzaldehyde was used instead of 2,5-dihydroxybenzaldehyde. Yield: 1.65 g (77%). m.p. 288–290 °C. $C_{10}H_{13}NO_4$ (211.2): calcd. C 56.8, H 6.2, N 6.6; found C 56.3, H 6.3, N 6.5. IR (KBr): $\tilde{\nu}$ = 3267 m (OH), 3085 m (NH); 1623 s $\upsilon_{as}(COO^-)$, 1522 s $\upsilon_s(COO^-)$, 1216 s (phenolic CO) cm^{-1}. ^{1}H NMR ([D$_6$]DMSO): δ = 1.29 (d, 3 H, -CH_3), 3.20 (m, 1 H, -CH), 3.91 (s, 2 H, benzylic), 7.01–6.21 (m, 3 H, Ar-H). ^{13}C NMR: δ = 15.4 ($CHCH_3$), 45.7 (benzylic), 56.6 (-$CHCH_3$), 116.1, 116.2, 117.0, 120.2, 148.7, and 149.5 (aromatic), 172.1 (-COOH). ESI-MS: *m*/*z* (%) = 211.3. $[\alpha]_D^{27}$: 8.0 (*c* = 5.5 mg mL^{-1}, MeOH).

***N*-(2,3-Dihydroxybenzyl)-L-alanine (H_3Diala3):** This ligand was prepared according to the same procedure as H_3Diala3 except that 2,3-dihydroxybenzaldehyde was used instead of 2,5-dihydroxybenzaldehyde. Yield: 1.41 g (66%). m.p. 262–264 °C. $C_{10}H_{13}NO_4$ (211.2): calcd. C 56.8, H 6.2, N 6.6; found C 56.7, H 6.0, N 6.4. IR (KBr): $\tilde{\nu}$ = 3367 m (OH), 3085 m (NH), $\upsilon_{as}(COO^-)$ 1623 s, 1522 s $\upsilon_s(COO^-)$, 1216 s (phenolic CO) cm^{-1}. ^{1}H NMR ([D$_6$]DMSO): δ = 1.30 (d, 3 H, -CH_3), 3.26 (m, 1 H, -CH), 3.96 (s, 2 H, benzylic), 6.78–6.62 (m, 3 H, aromatic). ^{13}C NMR: δ = 15.5 ($CHCH_3$), 45.8 (benzylic), 56.7 (-$CHCH_3$), 116.1, 116.2, 116.4, 120.6, 148.3, and 149.1 (aromatic), 170.5 (-COOH). ESI-MS: *m*/*z* (%) = 211.2. $[\alpha]_D^{27}$: 8.4 (*c* = 5.5 mg mL^{-1}, MeOH).

Complexes

The compound **[Cu_2(Scp11)$_2$(H_2O)$_2$] (1)** was synthesized according to the procedure described earlier.[6c] Weight loss (60–115 °C) as per TGA: 5.1% [calculated for 2 H_2O: 5.7%]. μ_B = 1.55 B. M. Slow diffusion of methanol into a slightly turbid solution of **1** in water afforded single crystals of [Cu_2(Scp11)$_2$(MeOH)$_2$] (**1a**).

[Cu_2(ClScp11)$_2$(H_2O)$_2$] (2): A clear solution containing of H_2Clscp11 (0.13 g, 0.5 mmol) and NaOH (0.04 g, 1.0 mmol) in methanol (20 mL) was obtained after stirring the mixture for 15 min. To this was added solid copper(II) acetate monohydrate in portions (0.10 g, 0.5 mmol). After stirring for another 2 h, a green solid separated out and was filtered off, washed with methanol (4 mL), diethyl ether (4 mL), and then in air. Yield: 0.31 g (88%). $C_{26}H_{32}Cl_2Cu_2N_2O_8$ (698.5): calcd. C 44.7, H 4.6, N 4.0; found C 45.1, H 4.7, N 3.7. IR (KBr): $\tilde{\nu}$ = 3400 m (OH), 2955 m (NH), 1619 s $\upsilon_{as}(COO^-)$, 1375 s $\upsilon_s(COO^-)$, 1266 s (phenolic CO) cm^{-1}. Weight loss (65–145 °C) as per TGA: 5.5% [calculated for 2 H_2O: 5.2%]. μ_B = 1.64 BM. Slow diffusion of acetonitrile into a saturated solution of **2** in DMF furnished dark green single crystals of [Cu_2(ClScp11)$_2$(DMF)(H_2O)]·MeCN (**2a**).

[Cu_2(MeScp11)$_2$(H_2O)$_2$] (3): To a clear solution of H_2MeScp11 (0.12 g, 0.5 mmol) and NaOH (0.04 g, 1.0 mmol) in a mixture of methanol (10 mL) and water (10 mL) was added copper(II) acetate monohydrate (0.10 g, 0.5 mmol) in portions. A green solid obtained after stirring for 2 h was filtered off, washed with water (2 × 2 mL), methanol (2 × 2 mL) and diethyl ether (2 × 2 mL) and then dried in air. Yield: 0.28 g (85%). $C_{28}H_{38}Cu_2N_2O_8$ (657.7): calcd. C 51.1, H 5.8, N 4.3; found C 51.2, H 5.9, N 4.1. IR (KBr): $\tilde{\nu}$ = 3399 m (OH), 2960 m (NH), 1621 s $\upsilon_{as}(COO^-)$, 1369 s $\upsilon_s(COO^-)$, 1264 s (phenolic CO) cm^{-1}. Weight loss (40–102 °C) as per TGA: 5.9% [calculated for 2 H_2O: 5.5%]. μ_B = 1.43 BM. Slow diffusion of methanol into a saturated solution of **3** in DMSO afforded single crystals of [Cu_2(MeScp11)$_2$(MeOH)$_2$]·2MeOH (**3a**).

[Cu_2(OHScp11)$_2$(H_2O)$_2$] (4): A suspension of H_2(OH)Scp11 (0.04 g, 0.16 mmol) in methanol (6 mL) was allowed to slowly diffuse into a clear solution of copper(II) acetate monohydrate (0.03 g, 0.16 mmol) in water (3 mL) in a test tube. Dark brownish green single crystals of **4** were obtained after 2 days. Yield: 76% (0.08 g). $C_{26}H_{34}Cu_2N_2O_{10}$ (661.6): calcd. C 47.2, H 5.2, N 4.2; found C 47.1, H 5.2, N 4.2. IR (KBr): $\tilde{\nu}$ = 3481 m (OH), 2954 m (NH); 1625 s $\upsilon_{as}(COO^-)$, 1366 s $\upsilon_s(COO^-)$, 1264 s (phenolic CO) cm^{-1}. Weight loss (134–177 °C) as per TGA: 5.8% [calculated for 2 H_2O: 5.4%]. μ_B = 1.41 BM.

[Cu_2(Sch11)$_2$]·(H_2O) (5): To a clear solution of H_2Sch11 (0.12 g, 0.50 mmol) and NaOH (0.04 g, 1.0 mmol) in methanol (20 mL) was added a solution of copper(II) acetate monohydrate (0.10 g, 0.50 mmol) in methanol (5 mL) and the solution was stirred for 3 h. The resulting green product was filtered, washed with methanol (2 × 2 mL), diethyl ether (2 × 2 mL), and then dried in air. Yield: 0.06 g (90%). $C_{28}H_{36}Cu_2N_2O_7$ (639.7): calcd. C 52.6, H 5.7, N 4.4; found C 52.4, H 5.7, N 4.3. IR (KBr): $\tilde{\nu}$ = 3435 m (OH), 2930 m (N–H), 1640 s $\upsilon_{as}(COO^-)$, 1373 s, $\upsilon_s(COO^-)$, 1272 s (phenolic CO) cm^{-1}. Weight loss (33–99 °C) as per TGA: 2.7% [calculated for H_2O: 2.8%]. μ_B = 1.57 BM.

[Cu_2(ClSch11)$_2$(H_2O)$_2$] (6): To a clear solution of H_2ClSch11 (0.14 g, 0.50 mmol) and NaOH (0.04 g, 1.0 mmol) in methanol (20 mL) was added copper(II) acetate monohydrate (0.10 g, 0.5 mmol) and the solution was stirred for 1.5 h. The green product was filtered off, washed with methanol (2 × 2 mL), diethyl ether (2 × 2 mL), and then dried in air. Yield: 0.32 g (88%). $C_{28}H_{36}Cl_2Cu_2N_2O_8$ (726.6): calcd. C 46.3, H 5.0, N 3.9; found C

46.7, H 5.0, N 3.5. IR (KBr): $\tilde{\nu}$ = 3447 m (OH), 2937 m (N–H), 1622 s $\upsilon_{as}(COO^-)$, 1382 s $\upsilon_s(COO^-)$, 1266 s, (phenolic CO) cm^{-1}. Weight loss (65–168 °C) as per TGA: 4.4% [calculated for $2H_2O$: 4.9%]. μ_B = 1.32 BM. Slow diffusion of methanol into a saturated solution of **6** in DMSO afforded dark green single crystals of $[Cu_2(ClSch11)_2(MeOH)_2]\cdot 2MeOH$ (**6a**).

$[Cu_2(MeSch11)_2(H_2O)_2]$ (7): A clear solution of copper(II) acetate monohydrate in methanol (5 mL) was added to a clear solution containing a mixture of H_2MeSch11 (0.26 g, 1.0 mmol) and NaOH (0.08 g, 2.00 mmol) in methanol (20 mL). Upon stirring this reaction mixture for 1.5 h, the resulting greenish product obtained was filtered, washed with methanol (4 mL), diethyl ether (4 mL), and then dried in air. Yield: 0.46 g (67%). $C_{30}H_{42}Cu_2N_2O_8$ (685.7): calcd. C 52.5, H 6.2, N 4.1; found C 53.2, H 6.2, N 4.1. IR (KBr): $\tilde{\nu}$ = 3436 m (OH), 2932 m (NH), 1624 s $\upsilon_{as}(COO^-)$, 1381 s $\upsilon_s(COO^-)$, 1262 s (phenolic CO) cm^{-1}. Weight loss (68–127 °C) as per TGA: 5.5% [calculated for $2H_2O$: 5.2%]. μ_B = 1.40 BM.

$[\{Cu_2(Sch12)_2\}_2Cu_2(Sch12)_2(H_2O)_2]\cdot 4H_2O$ (8): The ligand H_2Sch21 (0.12 g, 0.50 mmol) along with NaOH (0.04 g, 1.0 mmol) was added to a solvent mixture of water (15 mL) and acetonitrile (15 mL) and stirred for 15 min to obtain a clear solution. To this was added copper(II) nitrate trihydrate (0.12 g, 0.50 mmol) and the solution was stirred for another 3.5 h. The clear dark-green solution obtained was filtered. Dark green single crystals were formed from the clear filtrate upon slow evaporation for 4–5 days. Yield: 0.26 g (79%). $C_{84}H_{114}N_6O_{24}Cu_6$ (1973.1): calcd. C 51.1, H 5.8, N 4.3; found C 51.4, H 5.7, N 4.2. IR (KBr): $\tilde{\nu}$ = 3429 m (OH), 2928 m (NH), $\upsilon_{as}(COO^-)$ 1597 s 1360 s υ_s (COO^-), 1265 s (phenolic CO) cm^{-1}. Weight loss (64–119 °C) as per TGA: 5.9% [calculated for $6H_2O$: 5.5%]. μ_B = 1.31 BM.

$[Cu_2(ClSch12)_2]\cdot 2H_2O$ (9): To a clear solution of H_2ClSch12 (0.14 g, 0.5 mmol) and NaOH (0.04 g, 1.0 mmol) in methanol (10 mL) was added water (10 mL) followed by the addition solid copper(II) nitrate trihydrate (0.12 g, 0.5 mmol) and the mixture was stirred for 1.5 h. The dark green product obtained was filtered, washed with water (2 × 2 mL), methanol (2 × 2 mL) and diethyl ether (4 mL) and then dried in air. Yield: 0.31 g (85%). $C_{28}H_{36}Cl_2Cu_2N_2O_8$ (726.6): calcd. C 46.3, H 5.0, N 3.9; found C 47.0, H 5.2, N 4.0. IR (KBr): $\tilde{\nu}$ = 3396 m (OH), 3115 m (NH), 1603 s $\upsilon_{as}(COO^-)$, 1384 s $\upsilon_s(COO^-)$, 1264 s (phenolic CO) cm^{-1}. Weight loss (80–146 °C) as per TGA: 5.8% [calculated for $2H_2O$: 5.0%]. μ_B = 1.25 BM. A clear saturated solution of **9** in the solvent mixture of methanol/dichloromethane (1:1) afforded single crystals of $[Cu_2(ClSch12)_2]\cdot 2MeOH$, **9a** upon slow evaporation for 3 days.

$[Cu_2(MeSch12)_2(H_2O)_2]$ (10): A clear solution of H_2MeSch12 (0.26 g, 1.0 mmol) and NaOH (0.08 g, 2.0 mmol) in methanol (20 mL) was obtained on stirring the mixture for 15 min. To this was added solid copper(II) nitrate trihydrate (0.24 g, 1.0 mmol) in one portion. The reaction mixture was stirred for another 1 h. The greenish product obtained was filtered, washed with methanol, Et_2O, and then dried in air. Yield: 0.48 g (70%). $C_{30}H_{42}Cu_2N_2O_8$ (685.7): calcd. C 52.5, H 6.17, N 4.1; found C 52.4, H 6.25, N 4.1. IR (KBr): $\tilde{\nu}$ = 3458 m (OH), 2936 m (NH), 1601 s $\upsilon_{as}(COO^-)$, 1396 s $\upsilon_s(COO^-)$, 1262 s (phenolic CO) cm^{-1}. Weight loss (60–107 °C) as per TGA: 5.2% [calculated for $2H_2O$: 5.3%]. μ_B = 1.34 BM.

$[Cu_2(Diala5)_2(H_2O)_2]\cdot H_2O$ (11): To a clear solution of copper(II) acetate monohydrate (0.20 g, 1 mmol) in water (20 mL) H_3Diala5 (0.21 g, 1 mmol) was added directly and stirred for 3 h. The green solid obtained after stirring for 3 h was filtered, washed with methanol (2 × 2 mL), diethyl ether (2 × 2 mL), and then dried in air. Yield: 0.38 g (63%). $C_{20}H_{28}Cu_2N_2O_{11}$ (599.5): calcd. C 40.1, H 4.7, N 4.6; found C 40.2, H 4.8, N 4.2. IR (KBr): $\tilde{\nu}$ = 3406 m (OH), 2920 m (NH), 1611 s $\upsilon_{as}(COO^-)$, 1462 s $\upsilon_s(COO^-)$, 1299 s (phenolic CO) cm^{-1}. $[a]_D^{27}$: 97.4 (c = 5.5 mgmL^{-1}, DMSO). Weight loss (24–101 °C) as per TGA: 8.6% [calculated for $3H_2O$: 9.0%]. μ_B = 1.51 BM.

$[Cu_2(Diala4)_2(H_2O)_2]\cdot H_2O$ (12): To the clear solution of copper acetate (0.20 g, 1 mmol) in methanol (20 mL) H_3Diala4 (0.21 g, 1 mmol) was added directly and stirred. The green precipitate that formed after 10 min was subjected to further stirring for 3.5 h and then filtered off, washed with methanol, Et_2O, and dried in air. Yield: 0.36 g (61%). $C_{20}H_{28}Cu_2N_2O_{11}$ (599.5): calcd. C 40.1, H 4.7, N 4.6; found C 40.1, H 4.5, N 4.4. IR (KBr): $\tilde{\nu}$ = 3406 m (OH), 2920 m (NH), 1611 s $\upsilon_{as}(COO^-)$, 1462 s $\upsilon_s(COO^-)$, 1299 s (phenolic CO) cm^{-1}. $[a]_D^{27}$: 32.4 (c = 5.5 mgmL^{-1}, DMSO). Weight loss (23–106 °C) as per TGA: 8.2% [calculated for $3H_2O$: 9.0%]. μ_B = 1.25 BM. Slow diffusion of acetone into a saturated solution of **12** in DMSO afforded dark-green single crystals of $[Cu_2(Diala4)_2(DMSO)_2]\cdot 2DMSO\cdot 2$acetone (**12a**).

$[Cu_2(Diala3)_2(H_2O)_2]\cdot H_2O$ (13): To a clear solution of copper acetate (0.40 g, 2 mmol) in methanol (30 mL) H_3Diala3 (0.42 g, 2 mmol) was added directly and stirred. The dark-green solution was stirred for 5 h. The mixture was reduced to a small volume and then precipitated with excess of diethyl ether. The green product was dried in air. Yield: 0.82 g (68%). $C_{20}H_{28}Cu_2N_2O_{11}$ (599.5): calcd. C 40.1, H 4.7, N 4.6; found C 40.0, H 4.6, N 4.4. IR (KBr): $\tilde{\nu}$ = 3406 m (OH), 2920 m (NH), 1611 s $\upsilon_{as}(COO^-)$, 1462 s $\upsilon_s(COO^-)$; 1299 s (phenolic CO) cm^{-1}. $[a]_D^{27}$: 40.7 (c = 5.5 mgmL^{-1}, DMSO). Weight loss (80–131 °C) as per TGA: 8.6% [calculated for $3H_2O$: 9.0%]. μ_B = 1.91 BM.

Catecholase Activity and Kinetics Measurements: The catecholase activity of the complexes **1**–**13** described here in has been measured by the reaction with model substrate 3,5-DTBC at 25 °C. The growth of absorption maximum at λ_{max} = 390 nm, characteristic of the product of oxidation 3, 5-DTBQ, was measured as a function of time. For this purpose, 10^{-4} moldm^{-3} solutions of **1**–**13** were treated with 50 equivalents of 3,5-DTBC. The reaction was carried out in methanol because of the satisfactory solubility of 3,5-DTBC and 3,5-DTBQ. The course of the reaction was followed by UV/Vis spectroscopy. The UV/Vis spectra of the original solution directly after the addition and after 10, 20, 30, 40, 50, 60, 75, 90, 105, and 120 min were recorded and corrected for volume changes. The increase in the absorption due to the formation of DTBQ at 390 nm indicated significant catalytic activity for all the complexes. Kinetic parameters on the rate of catechol oxidation were determined by reaction of $1\,10^{-3}$ to $1.3\,10^{-2}$ M solutions of DTBC with 10^{-4} solutions of complexes in methanol. A kinetic treatment on the basis of the Michaelis–Menten approach was applied and the results were evaluated from Lineweaver–Burk double reciprocal plots. The errors in the kinetic parameters were obtained from at least three measurements.

X-ray Crystallography: The diffraction experiments were carried out with a Bruker AXS SMART CCD diffractometer. The program SMART[34a] was used for collecting frames of data, indexing reflections, and determining lattice parameters, SAINT[34a] for integration of the intensity of reflections and scaling, SADABS[34b] for absorption correction and SHELXTL[34c] for space group and structure determination, least-squares refinements on F^2. All the hydrogen atom positions of the imine groups, methanol, and water molecules were located and their positional parameters were refined in the least-squares cycles. One of the carbon atoms in **2a** (C12 with occupancies 0.65/0.35) and **3a** (C11 with occupancies 0.6/0.4) were found to be disordered. Selected crystallographic data

Table 5. X-ray crystallographic data and structure refinement details.

Complex	**1a**	**2a**	**3a**	**4**
Formula	$C_{28}H_{38}Cu_2N_2O_8$	$C_{31}H_{40}Cl_2Cu_2N_4O_8$	$C_{32}H_{50}Cu_2N_2O_{10}$	$C_{26}H_{34}Cu_2N_2O_{10}$
Formula wt.	657.68	794.65	749.82	661.63
T [K]	223(2)	223(2)	223(2)	223(2)
Crystal system	monoclinic	triclinic	triclinic	triclinic
Space group	$C2/c$	$P\bar{1}$	$P\bar{1}$	$P\bar{1}$
a [Å]	16.5064(8)	11.2530(6)	7.7219(5)	7.7024(8)
b [Å]	14.5462(7)	12.3363(7)	10.4139(7)	8.8514(9)
c [Å]	14.1803(7)	13.9093(8)	11.599(28)	9.835(1)
α [°]	90	107.662(1)	106.958(1)	76.240(2)
β [°]	124.930	105.555(1)	106.312(1)	89.220(2)
γ [°]	90	98.783(1)	96.710(1)	81.352(2)
V [Å^3]	2791.4(2)	1713.9(2)	836.0(1)	643.7(1)
Z	4	2	1	1
μ [mm^{-1}]	1.577	1.451	1.331	1.716
Reflections collected	8047	9753	4902	3806
Independent reflections	2460	5943	2948	2266
R_{int}	0.0313	0.0196	0.0135	0.0164
GooF	1.010	1.034	1.054	1.053
Final R [$I>2\sigma$], R_1[a]	0.0372	0.0479	0.0316	0.0337
wR_2[b]	0.0902	0.1212	0.0828	0.0831
Complex	**6a**	**8**	**9a**	**12a**
Formula	$C_{32}H_{48}Cl_2Cu_2N_2O_{10}$	$C_{28}H_{38}Cu_2N_2O_8$	$C_{30}H_{40}Cl_2Cu_2N_2O_8$	$C_{34}H_{58}Cu_2N_2O_{14}S_4$
Formula wt.	817.7	657.68	754.62	974.14
T [K]	223(2)	223(2)	223(2)	223(2)
Wavelength [Å]	0.71073	0.71073	0.71073	0.71073
Crystal system	triclinic	triclinic	triclinic	triclinic
Space group	$P\bar{1}$	$P\bar{1}$	$P\bar{1}$	$P1$
a [Å]	7.7614(3)	12.3573(11)	7.4698(9)	9.5244(7)
b [Å]	10.8014(4)	14.1055(14)	9.9411(12)	10.8149(8)
c [Å]	11.8232(4)	14.1822(15)	11.2134(14)	12.0257(9)
α [°]	108.395(2)	104.195(2)	72.522(3)	96.841(2)
β [°]	107.969(2)	110.017(2)	79.596(3)	102.547(2)
γ [°]	95.718(2)	104.945(3)	88.363(3)	111.801(2)
V [Å^3]	873.10(6)	2087.2(4)	780.9(2)	1095.0(1)
Z	1	3	1	1
μ [mm^{-1}]	1.429	1.582	1.586	1.225
Reflections collected	7693	17670	6432	6278
Independent reflections	5003	10780	4305	4545
R_{int}	0.0206	0.0239	0.0216	0.0162
GooF	0.921	1.019	1.084	1.078
Final R [$I > 2\sigma$], R_1[a]	0.0398	0.0376	0.0521	0.0444
wR_2[a]	0.0856	0.0734	0.1146	0.1136

[a] $R_1 = \Sigma||F_o| - |F_c||/\Sigma|F_o|$. [b] $wR_2 = [\Sigma w(F_o^2 - F_c^2)^2/\Sigma w(F_o^2)^2]^{1/2}$.

and refinement details are displayed in Table 5. The structure of **12a** can also be solved in the centrosymmetric space group $P\bar{1}$ with the methyl group of the alanine part of the ligand disordered. However, the optical activity of **12** containing the optically active Diala4 ligand is comparable to those of **11** and **13** and therefore, the chiral space group was retained.

CCDC-277306 to -277313 (for **1a**, **2a**, **3a**, **4**, **6a**, **8**, **9a**, and **12a**, respectively) contain the supplementary crystallographic data discussed in this paper. These data can be obtained free of charge from The Cambridge Crystallographic Data Centre via www.ccdc.cam.ac.uk/data_request/cif.

Supporting Information (see also the footnote on the first page of this article): Structure diagrams, thermogravimetric curves, UV/Vis spectra of the oxidation of 3,5-DTBC, Lineweaver–Burk plots (1/v vs. 1/[S]) and ESI-MS data (total number of pages: 25).

Acknowledgments

We gratefully acknowledge the financial support from NUS (R143-000-252-112), and from NSFC (20125104, 20490210).

[1] a) H. S. Mason, *Nature* **1956**, *177*, 79–81; b) J. R. Walker, P. H. Ferrar, *Biotechnol. Genet. Eng. Rev.* **1998**, *15*, 457–498; c) R. H. Holm, E. I. Solomon, *Chem. Rev.* **1996**, *96*, 2239–3042.

[2] a) C. X. Zhang, H.-C. Liang, K. J. Humphreys, K. D. Karlin in *Advances in Catalytic Activation of Dioxygen by Metal Complexes* (Ed.: L. I. Simandi), Kluwer Academic Publishers, Dordrecht, **2003**, pp. 79–121; b) K. D. Karlin, Z. Tyeklar, *Bioinorganic Chemistry of Copper*, Chapman & Hall, New York, **1993**.

[3] a) C. Gerdermann, C. Eicken, B. Krebs, *Acc. Chem. Res.* **2002**, *35*, 183–191; b) C. Eicken, F. Zippel, K. Buldt-Karentzopoulos, B. Krebs, *FEBS Lett.* **1998**, *436*, 293–299.

[4] a) E. I. Solomon, U. M. Sundaram, T. E. Machonkin, *Chem. Rev.* **1996**, *96*, 2563–2605; b) W. B. Tolman, *Acc. Chem. Res.* **1997**, *30*, 227–237; c) E. A. Lewis, W. B. Tolman, *Chem. Rev.* **2004**, *104*, 1047–1076; d) L. M. Miricia, X. Ottenwaelder, T. D. P. Stack, *Chem. Rev.* **2004**, *104*, 1013–1045; e) L. Q. Hatcher, K. D. Karlin, *J. Biol. Inorg. Chem.* **2004**, *9*, 669–683; f) A. L. Gavrilova, B. Bosnich, *Chem. Rev.* **2004**, *104*, 349–383.

[5] See for example, a) K. D. Karlin, *Science* **1993**, *261*, 701–708; b) J. Reedjik, *Bioinorganic Catalysis* (Ed.: J. Reedjik), 2nd ed., Dekker, New York, **1999**; c) T. N. Sorrell, *Tetrahedron* **1989**, *45*, 3–68; d) P. A. Vigato, S. Tamburini, D. E. Fenton, *Coord. Chem. Rev.* **1990**, *106*, 25–170; e) N. Kitajima, *Adv. Inorg. Chem.* **1992**, *39*, 1–77; f) P. Gentschev, M. Luken, N. Moller, A. Rompel, B. Krebs, *Inorg. Chem. Commun.* **2001**, *4*, 753–756; g) R. Wegner, M. Dubs, H. Gorls, C. Robl, B. Schonecker, E.-G. Jager, *Steroids* **2002**, *67*, 835–849; h) R. Wegner, M. Gottschaldt, P. Wolfgang, E.-G. Jager, D. Klemm, *J. Mol. Catal. A* **2003**, *201*, 93–118 and references cited therein; i) C. Belle, J. L. Pierre, *Eur. J. Inorg. Chem.* **2003**, 4137–4146; j) B. Krebs, M. Merkel, A. Rompel, *J. Argent. Chem. Soc.* **2004**, *92*, 1–15 and references cited therein; k) J. Kaizer, R. Csonka, G. Speir, M. Giorgi, M. Reglier, *J. Mol. Catal. A* **2005**, *235*, 81–87; l) C. H. Lee, S. T. Wong, T. S. Lin, C. Y. Mou, *J. Phys. Chem. B* **2005**, *109*, 775–784; m) I. A. Koval, C. Belle, K. Selmeczi, C. Philouze, S. A. Eric, A. M. Schuitema, P. Gamez, J. L. Pierre, J. Reedjik, *J. Biol. Inorg. Chem.* **2005**, *10*, 739–750.

[6] a) J. D. Ranford, J. J. Vittal, D. Wu, *Angew. Chem. Int. Ed. Engl.* **1998**, *37*, 1114–1116; b) J. D. Ranford, J. J. Vittal, D. Wu, X. Yang, *Angew. Chem. Int. Ed.* **1999**, *38*, 3498–3501; c) B. Sreenivasulu, J. J. Vittal, *Crystal Growth Des.* **2003**, *3*, 635–637.

[7] B. Sreenivasulu, J. J. Vittal, *Angew. Chem. Int. Ed.* **2004**, *43*, 5769–5772.

[8] C. T. Yang, M. Vetrichelvan, X. D. Yang, B. Moubaraki, K. S. Murray, J. J. Vittal, *Dalton Trans.* **2004**, 113–121.

[9] B. Sreenivasulu, M. Vetrichelvan, F. Zhao, S. Gao, J. J. Vittal, *Eur. J. Inorg. Chem.* **2005**, 4635–4645.

[10] a) C. Belle, C. Beguin, I. Gautier-Luneau, S. Hamman, C. Philouze, J. L. Pierre, F. Thomas, S. Torelli, E. Saint-Aman, M. Bonin, *Inorg. Chem.* **2002**, *41*, 479–491; b) S. Mukherjee, T. Weyhermuller, E. Bothe, K. Weighardt, P. Chaudhuri, *Dalton Trans.* **2004**, 3842–3853.

[11] a) G. B. Deacon, R. Philips, *Coord. Chem. Rev.* **1980**, *33*, 227–250; b) C. Djordjevic, M. Lee, E. Sinn, *Inorg. Chem.* **1989**, *28*, 719–723; c) J. R. Ferraro, *Low-frequency Vibrations of Inorganic and Coordination compounds*, Plenum Press, New York, **1971**; d) D. A. Edwards, R. N. Hayward, *Can. J. Chem.* **1968**, *46*, 3443–3446.

[12] K. Nakamato, *Infrared and Raman Spectra of Inorganic and Coordination Compounds*, 4th ed., John Wiley & Sons, New York, **1986**, pp. 191–371.

[13] a) L. Sacconi, M. Ciampolini, *J. Chem. Soc.* **1964**, 276–280; b) A. B. P. Lever, *Inorganic Electronic Spectroscopy*, Elsevier, New York, **1968**.

[14] a) A. B. P. Lever, *Inorganic Electronic Spectroscopy*, Elsevier, Amsterdam, **1984**; pp. 553–572; b) C. T. Yang, B. Moubaraki, K. S. Murray, J. D. Ranford, J. J. Vittal, *Inorg. Chem.* **2001**, *40*, 5934–5941; c) W. Mazurek, B. J. Kennedy, K. S. Murray, M. J. O'Connor, J. R. Rodger, M. R. Snow, A. G. Wedd, P. R. Zwak, *Inorg. Chem.* **1985**, *24*, 3258–3264; d) R. C. Holz, J. M. Brink, F. T. Gobena, C. J. O'Connor, *Inorg. Chem.* **1994**, *33*, 6086–6092; e) B. Bleaney, K. D. Bowers, *Proc. R. Soc. A* **1952**, *214*, 451–465; f) O. Kahn, *Molecular Magnetism*, VCH, New York, **1993**.

[15] a) A. W. Addison, T. N. Rao, J. Reedijk, J. V. Rijn, G. C. Verschoor, *J. Chem. Soc., Dalton Trans.* **1984**, 1349–1356; b) G. Murphy, C. O. Sullivan, B. Murphy, B. Hathaway, *Inorg. Chem.* **1998**, *37*, 240–248; c) D. S. Marlin, M. M. Olmstead, P. K. Mascharak, *Inorg. Chem.* **2001**, *40*, 7003–7008; d) C. T. Yang, J. J. Vittal, *Inorg. Chim. Acta* **2003**, *344*, 65–76, and references therein.

[16] a) B. F. Hoskins, R. Robson, *J. Am. Chem. Soc.* **1990**, *112*, 1546–1554; b) R. W. Gable, B. F. Hoskins, R. Robson, *J. Chem. Soc., Chem. Commun.* **1990**, 1677–1678; c) M. J. Zaworotko, *Chem. Commun.* **2001**, 1–9; d) B. Moulton, M. J. Zaworotko, *Chem. Rev.* **2001**, *101*, 1629–1658; e) A. N. Khlobystov, A. J. Blake, N. R. Champness, D. A. Lemenovskii, A. G. Majouga, N. V. Zyk, M. Schröder, *Coord. Chem. Rev.* **2001**, *222*, 155–192; f) B. Kumar, M. Fujita, *J. Chem. Soc., Dalton Trans.* **2000**, 3805–3810; g) L. Carlucci, G. Ciani, D. M. Proserpio, *New J. Chem.* **1998**, *22*, 1319–1321; h) S. R. Bettens, R. Robson, *Angew. Chem. Int. Ed. Engl.* **1998**, *37*, 1460–1494; i) S. R. Bettens, B. F. Hoskins, R. Robson, *Chem. Eur. J.* **2000**, *6*, 156–161; j) S. R. Bettens, *CrystEngComm* **2001**, *3*, 67–73.

[17] a) G. R. Desiraju, *Crystal Engineering: The Design of Organic Solids*, Elsevier, Amsterdam, **1989**; b) G. R. Desiraju, *Acc. Chem. Res.* **2002**, *35*, 565–573; c) C. B. Aakeroy, A. M. Beatty, D. S. Leinen, *Angew. Chem. Int. Ed.* **1999**, *38*, 1815–1819; d) A. M. Beatty, *CrystEngComm* **2001**, *51*, 1–15; e) J. K. Craig, M. S. S. Janet, L. W. James, M. S. V. W. Solange, N. L. John, C. Glidewell, *Acta Crystallogr., Section B* **2002**, *58*, 94–108; f) T. Steiner, *Angew. Chem. Int. Ed.* **2002**, *41*, 48–76.

[18] a) A. B. P. Lever, B. S. Ramaswamy, S. R. Pickens, *Inorg. Chim. Acta* **1980**, *46*, L59–61; b) T. R. Demmin, M. D. Swerdloff, M. M. Rogic, *J. Am. Chem. Soc.* **1981**, *103*, 5795–5804; c) F. Zippel, F. Ahlers, R. Werner, W. Haase, H.-F. Nolting, B. Krebs, *Inorg. Chem.* **1996**, *35*, 3409–3419; d) Y.-H. Chung, H.-H. Wei, Y.-H. Liu, G.-H. Lee, Y. Wang, *J. Chem. Soc., Dalton Trans.* **1997**, 2825–2829; e) R. Wegner, M. Gottschaldt, H. Gorls, E.-G. Jager, D. Klemm, *Angew. Chem. Int. Ed.* **2000**, *39*, 595–599; f) R. Wegner, M. Gottschaldt, H. Gorl, E.-G. Jager, D. Klemm, *Chem. Eur. J.* **2001**, *7*, 2143–2157; g) P. Gentschev, N. Moller, B. Krebs, *Inorg. Chim. Acta* **2000**, *300–302*, 442–452; h) M. Merkel, N. Moller, M. Piacenza, S. Grimme, A. Rompel, B. Krebs, *Chem. Eur. J.* **2005**, *11*, 1201–1209; i) I. A. Koval, D. Pursche, A. F. Stassen, P. Gamez, B. Krebs, J. Reedijk, *Eur. J. Inorg. Chem.* **2003**, 1669–1674.

[19] For mononuclear complexes see: a) N. Oshi, Y. Nishida, K. Ida, S. Kida, *Bull. Chem. Soc. Jpn.* **1980**, *53*, 2847–2850; b) U. Casellato, S. Tamburini, P. A. Vigato, A. de Stefani, M. Vidali, D. E. Fenton, *Inorg. Chim. Acta* **1983**, *69*, 45–51; c) M. R. Malachowski, M. G. Davidson, *Inorg. Chim. Acta* **1989**, *162*, 199–204; d) C.-H. Kao, H.-H. Wie, Y.-H. Liu, G.-H. Lee, Y. Wang, C.-J. Lee, *J. Inorg. Biochem.* **2001**, *84*, 171–178.

[20] For redox potentials of catechols see: a) L. Horner, E. Geyer, *Chem. Ber.* **1965**, *98*, 2016–2045; b) S. Harmalker, S. E. Jones, D. T. Sawyer, *Inorg. Chem.* **1983**, *22*, 2790–2794; c) J. Rall, M. Wanner, M. Albrecht, F. M. Hornung, W. Kaim, *Chem. Eur. J.* **1999**, *5*, 2802–2808.

[21] a) A. Rompel, H. Fischer, D. Meiwes, K. Buldt-Karentzoloulos, R. Dillinger, F. Tuczek, H. Witzel, B. Krebs, *J. Biol. Inorg. Chem.* **1999**, *4*, 56–63; b) T. Klabunde, C. Eicken, J. C. Sacchettini, B. Krebs, *Nat. Struct. Biol.* **1998**, *5*, 1084–1090; c) C. Eicken, B. Krebs, J. C. Sacchettini, *Curr. Opin. Struct. Biol.* **1999**, *9*, 677–683.

[22] a) K. D. Karlin, M. S. Nasin, B. I. Cohen, R. W. Cruse, S. Kaderli, A. D. Zuberbuhler, *J. Am. Chem. Soc.* **1994**, *116*, 1324–1336; b) K. D. Karlin, N. Wei, B. Jung, S. Kaderli, P. Niklaus, A. D. Zuberbuhler, *J. Am. Chem. Soc.* **1993**, *115*, 9506–9514; c) G. Battaini, E. Monzani, L. Casella, L. Santagostini, R. Pagliarin, *J. Biol. Inorg. Chem.* **2000**, *5*, 262–268.

[23] a) M. Thirumavalavan, P. Akilan, M. Kandaswamy, *Supramol. Chem.* **2004**, *16*, 137–146; b) M. R. Malachowski, B. Dorsey, J. G. Sackett, R. S. Kelly, A. L. Ferko, R. N. Hardin, *Inorg. Chim. Acta* **1996**, *249*, 85–92; c) M. R. Malachowski, J. Carden, M. G. Davidson, W. L. Driessen, J. Reedijk, *Inorg. Chim. Acta* **1997**, *257*, 59–67.

[24] a) S. Torelli, C. Belle, I. Gautier-Luneau, J. L. Pierre, E. Saint-Aman, J. M. Latour, L. Le Pape, D. Luneau, *Inorg. Chem.* **2000**, *39*, 3526–3536; b) C. Fernandes, A. Neves, A. J. Bortoluzzi, A. S. Mangrich, E. Rentschler, B. Szpoganicz, E. Schwin-

gel, *Inorg. Chim. Acta* **2001**, *320*, 12–21; c) C.-H. Kao, H.-H. Wie, Y.-H. Liu, G.-H. Lee, Y. Wang, C.-J. Lee, *Inorg. Biochem.* **2001**, *84*, 171–178; d) R. Than, A. A. Feldman, B. Krebs, *Coord. Chem. Rev.* **1999**, *182*, 211–241.

[25] a) J. Mukherjee, R. Mukherjee, *Inorg. Chim. Acta* **2002**, *337*, 429–438; b) A. Neves, L. M. Rossi, A. J. Bortoluzzi, B. Szpoganicz, C. Wiezbicki, E. Schwingel, W. Haase, S. Ostrovsky, *Inorg. Chem.* **2002**, *41*, 1788–1794; c) O. Seneque, M. Campion, B. Douziech, M. Giorgi, E. Riviere, Y. Journaux, Y. L. Mest, O. Reinaud, *Eur. J. Inorg. Chem.* **2002**, 2007–2014.

[26] a) K. D. Karlin, S. Kaderli, A. D. Zuberbuhler, *Acc. Chem. Res.* **1997**, *30*, 139–147; b) N. Kitajima, Y. Moro-oka, *Chem. Rev.* **1994**, *94*, 737–757; c) E. I. Solomon, F. Tuczek, D. E. Root, C. A. Brown, *Chem. Rev.* **1994**, *94*, 827–856.

[27] J. Ackermann, F. Meyer, E. Kaifer, H. Pritzkow, *Chem. Eur. J.* **2002**, *8*, 247–258.

[28] J. Reim, B. Krebs, *J. Chem. Soc., Dalton Trans.* **1997**, 3793–3804.

[29] J. McMurray, *Organic Chemistry*, Brooks/Cole, Monterey, California, 3rd ed., **1992**.

[30] a) J. P. Chyn, F. L. Urbach, *Inorg. Chim. Acta* **1991**, *189*, 157–163; b) J. Balla, T. Kiss, R. F. Jameson, *Inorg. Chem.* **1992**, *31*, 58–62; c) K. Selmeczi, M. Reglier, M. Giorgi, G. Speier, *Coord. Chem. Rev.* **2003**, *245*, 191–201.

[31] a) E. Monzani, L. Quinti, A. Perotti, L. Casella, M. Gullotti, L. Randaccio, S. Geremia, G. Nardin, P. Faleschini, G. Tabbi, *Inorg. Chem.* **1998**, *37*, 553–562; b) E. Monzani, G. Battaini, A. Perotti, L. Casella, M. Gullotti, L. Santagostini, G. Nardin, L. Randaccio, S. Geremia, P. Zanello, G. Opromolla, *Inorg. Chem.* **1999**, *38*, 5359–5369.

[32] a) A. Granata, E. Monzani, L. Casella, *J. Biol. Inorg. Chem.* **2004**, *9*, 903–913.

[33] C. Eicken, C. Gerdemann, B. Krebs, in: *Handbook of Metalloproteins* (Ed.: A. Messerschmidt), John Wiley & Sons, Chichester, **2001**, vol. 2, pp. 1319–1329.

[34] a) *SMART* & *SAINT* Software Reference Manuals, Version 6.22, Bruker AXS Analytic X-ray Systems, Inc., Madison, WI, **2000**; b) G. M. Sheldrick, *SADABS*, Software for Empirical Absorption Correction, University of Gottingen, Germany, **2000**; c) *SHELXTL* Reference Manual, Version 5.1, Bruker AXS, Analytic X-ray Systems, Inc., Madison, WI, **1997**.

Received: January 11, 2006
Published Online: April 26, 2006

